RESEARCH ARTICLE

Key Points:
- Simulated midnineteenth century ozone distribution is sensitive to assumed model vegetation distribution
- Impact of midnineteenth century to present day vegetation change on tropospheric ozone dominated by change in isoprene emissions
- Ozone radiative forcing is sensitive to assumption regarding midnineteenth century vegetation distribution

Correspondence to:
S. R. Arnold,
s.arnold@leeds.ac.uk

Sensitivity of midnineteenth century tropospheric ozone to atmospheric chemistry-vegetation interactions

M. J. Hollaway[1,2], **S. R. Arnold[1]**, **W. J. Collins[3,4]**, **G. Folberth[2]**, and **A. Rap[1]**

[1] Institute for Climate and Atmospheric Science, School of Earth and Environment, University of Leeds, Leeds, UK, [2] Now at Lancaster Environment Centre, Lancaster University, Lancaster, UK, [3] Hadley Centre, Met Office, Exeter, UK, [4] Now at Department of Meteorology, University of Reading, Reading, UK

Abstract We use an Earth System model (HadGEM2-ES) to investigate the sensitivity of midnineteenth century tropospheric ozone to vegetation distribution and atmospheric chemistry-vegetation interaction processes. We conduct model experiments to isolate the response of midnineteenth century tropospheric ozone to vegetation cover changes between the 1860s and present day and to CO_2-induced changes in isoprene emissions and dry deposition over the same period. Changes in vegetation distribution and CO_2 suppression of isoprene emissions between midnineteenth century and present day lead to decreases in global isoprene emissions of 19% and 21%, respectively. This results in increases in surface ozone over the continents of up to 2 ppbv and of 2–6 ppbv in the tropical upper troposphere. The effects of CO_2 increases on suppression of isoprene emissions and suppression of dry deposition to vegetation are small compared with the effects of vegetation cover change. Accounting for present-day climate in addition to present-day vegetation cover and atmospheric CO_2 concentrations leads to increases in surface ozone concentrations of up to 5 ppbv over the entire northern hemisphere (NH) and of up to 8 ppbv in the NH free troposphere, compared with a midnineteenth century control simulation. Ozone changes are dominated by the following: (1) the role of isoprene as an ozone sink in the low NO_x midnineteenth century atmosphere and (2) the redistribution of NO_x to remote regions and the free troposphere via PAN (peroxyacetyl nitrate) formed from isoprene oxidation. We estimate a tropospheric ozone radiative forcing of 0.264 W m^{-2} and a sensitivity in ozone radiative forcing to midnineteenth century to present-day vegetation cover change of -0.012 W m^{-2}.

1. Introduction

Ozone in the troposphere is a secondary pollutant, which, in addition to being a greenhouse gas, is harmful to human health, increasing mortality [*Anenberg et al.*, 2010], and is damaging to ecosystems, reducing global crop yields [*Van Dingenen et al.*, 2009; *Hollaway et al.*, 2012; *Avnery et al.*, 2013; *Tai et al.*, 2014] and inhibiting the land carbon sink [*Sitch et al.*, 2007; *Collins et al.*, 2010; *Lombardozzi et al.*, 2013, 2015; *Yue and Unger*, 2014]. Since the midnineteenth century period, anthropogenic emissions of ozone precursors (NO_x, CO, CH_4, and volatile organic compounds (VOCs)) have led to increased tropospheric ozone, particularly over industrialized northern hemisphere (NH) regions [*Stevenson et al.*, 2013]. Model calculations estimate the radiative forcing due to this increase in tropospheric ozone to be 0.4± 0.2 (95% confidence limit) W m^{-2} [*Myhre et al.*, 2013]. Uncertainty on this value partly results from uncertainty in processes controlling ozone concentrations in the pre-industrial, which define the baseline on top of which anthropogenic ozone precursor sources contribute. Such uncertainties include assumptions regarding midnineteenth century emissions of ozone precursors from natural sources such as biomass burning and lightning [*Mickley et al.*, 2001] and differences between present-day and pre-industrial climate, which affect meteorology and transport. Uncertainties in biogenic foliage emissions, soil NO_x emissions, and the available land cover maps could also potentially contribute to the uncertainty in modeled pre-industrial ozone concentrations.

Mickley et al. [2001] showed that reducing NO_x emissions from lightning and soils and increasing the emission of biogenic hydrocarbons can produce lower ozone concentrations in the pre-industrial, compared to a baseline scenario where these precursor sources were held at present-day levels. This resulted in a much higher revised radiative forcing of 0.72–0.80 W m^{-2} compared to 0.44 W m^{-2} in the baseline case. This increased forcing range is substantially larger than the more recent estimates from *Myhre et al.* [2013] and those from the

Atmospheric Chemistry and Climate Intercomparison Project (ACCMIP) (0.29–0.53 W m^{-2}) [*Stevenson et al.*, 2013]. The most likely reason for the larger estimate of *Mickley et al.* [2001] is due to different assumptions in precursor emissions and the off-line reduction in biogenic emissions. Uncertainties associated with the representation of inorganic bromine (Br$_y$) chemistry [*Parrella et al.*, 2012] and the magnitude of biomass burning in the midnineteenth century period [*Wang and Jacob*, 1998; *Shindell et al.*, 2003; *Lamarque et al.*, 2005; *Rap et al.*, 2015] also lead to poor constraint on the pre-industrial ozone distribution. This is demonstrated by the findings of *Rap et al.* [2015] where the introduction of present-day biomass burning emissions in the pre-industrial produced a reduction in the calculated ozone radiative forcing from 0.32 W m^{-2} to 0.23 W m^{-2}.

Additional influences on the change between pre-industrial and present-day tropospheric ozone also result from changes in land cover. Emissions of biogenic volatile organic compounds (BVOCs), such as isoprene, are highly sensitive to vegetation type and foliage density (leaf area index) [*Niinemets et al.*, 2010a, 2010b; *Guenther et al.*, 2006], as well as environmental controls such as light [*Monson and Fall*, 1989; *Strada and Unger*, 2016], temperature [*Guenther et al.*, 1993], atmospheric CO_2 [*Monson et al.*, 2007], and soil moisture [*Pegoraro et al.*, 2004; *Monson et al.*, 2007]. The rate of isoprene emission increases with temperature until an optimum of about 40°C [*Niinemets et al.*, 1999]; however, evidence suggests that this can vary between plant species and can be affected by plants becoming acclimatized to their conditions [*Wilkinson et al.*, 2009; *Niinemets and Sun*, 2015]. Conversely, measurements have shown that increased ambient CO_2 concentrations inhibit isoprene emission [*Possell et al.*, 2005; *Wilkinson et al.*, 2009], with the potential of different response patterns to short- and long-term changes in the atmospheric CO_2 burden [*Young et al.*, 2009; *Pacifico et al.*, 2009]. Accordingly, changes in vegetation distributions and environmental drivers between midnineteenth century and present day are expected to result in changes in the distribution and magnitude of global isoprene emissions. Changes in both the magnitude and spatial distribution of isoprene emissions can lead to enhanced ozone production or enhanced ozone loss, depending on the local NO$_x$ burden [*Sillman*, 2000; *Ryerson et al.*, 2001; *Arneth et al.*, 2007]. A recent study attributed a substantial negative ozone radiative forcing (−0.13 W m^{-2}) to a reduction in forest tree cover since the pre-industrial and the associated decrease in isoprene emissions [*Unger*, 2014].

Isoprene oxidation in the presence of NO$_x$ can also result in the formation of peroxyacetylnitrate (PAN) which can act as reservoir species for NO$_x$ enabling long-range transport of reactive nitrogen, leading to ozone production in regions remote from ozone precursor emissions [*Wang et al.*, 1998]. Furthermore, in the tropics, where large isoprene sources may coincide with sources of NO$_x$ from biomass burning or lightning [*Guenther et al.*, 2006; *Lelieveld et al.*, 2008], the formation of PAN can coincide with areas of deep convection which can result in its rapid transportation to the free troposphere. Here temperatures are sufficiently low for PAN to remain stable and be transported over long distances [*Moxim et al.*, 1996] and further contribute to ozone production in remote regions. This implies a strong sensitivity of the large-scale impact of isoprene on tropospheric ozone to assumptions regarding NO$_x$ emissions.

Vegetation cover also has a significant impact on dry deposition. The dominant pathway for dry deposition loss of ozone, and its precursors, is uptake to vegetation, by direct uptake through plant stomata and deposition to the leaf cuticular surface [*Wesely*, 1989; *Smith et al.*, 2000]. Consequently, rates of dry deposition of ozone and its precursor species (including NO$_x$, PAN, and other reactive nitrogen species) are highly sensitive to land cover and treatments of model vegetation [*Ganzeveld and Lelieveld*, 1995; *Giannakopoulos et al.*, 1999; *Val Martin et al.*, 2014]. In addition, the ambient atmospheric CO_2 concentration can influence the rate of dry deposition due to higher CO_2 concentrations inducing stomatal closure and hence reducing the rate of trace gas exchange between the atmosphere and vegetation [*Gedney et al.*, 2006].

The effects of vegetation cover and CO_2 change on isoprene emissions and dry deposition, respectively, have been shown to have competing impacts on tropospheric ozone concentrations [*Wu et al.*, 2012; *Fu and Tai*, 2015]. For example, *Fu and Tai* [2015] demonstrated that in the high NO$_x$, VOC-limited regime over many parts of central China, despite increases in isoprene emissions, ozone concentrations were estimated to decrease. It was shown that elevated summertime leaf area index (LAI) enhanced dry deposition and thus dominated the small rise in ozone from enhanced isoprene. In contrast, in the NO$_x$-limited parts of western China, reductions in isoprene emissions were shown to dominate, and despite higher dry deposition over these regions, ozone levels were shown to increase [*Fu and Tai*, 2015]. Furthermore, it has been shown that the type of vegetation (e.g., forest versus cropland) and anthropogenic emissions changes can also play a strong role in determining

whether the isoprene or dry deposition effect dominates the response of modeled surface ozone to a change in vegetation cover [*Wu et al.*, 2012; *Fu and Tai*, 2015].

In this study, we use a coupled global Earth System (ES) model to investigate how changes in interactions between vegetation and atmospheric composition between 1865 and near present day (here defined as the year 2000) impact tropospheric ozone abundances and radiative forcing. The midnineteenth century is often assumed to define the pre-industrial period in tropospheric ozone studies, such as the ACCMIP exercise, where 1850 is used as pre-industrial [*Young et al.*, 2013]. We use a coupled land surface-atmospheric chemistry-climate configuration of the HadGEM2-ES model, which includes photosynthesis-driven biogenic VOC emissions from vegetation and explicitly links vegetation stomatal conductance to reactive trace-gas dry deposition. We separately assess the impacts of the 1865 to present day changes in land surface cover, climate, and atmospheric CO_2 on the dry deposition of ozone and its precursors, and biogenic isoprene emissions (fast responses due to impacts on photosynthesis rather than long-term responses due to changes in vegetation distribution), and the resultant effects on the simulated midnineteenth century tropospheric ozone distribution. The effect of these land cover-driven changes on the estimated midnineteenth century to present-day tropospheric ozone radiative forcing is also quantified. The HadGEM2-ES Earth System model and model scenarios are described in section 2. Section 3 presents the impacts of changing model atmospheric chemistry-vegetation interactions on atmospheric composition, focusing on tropospheric ozone and its precursor species. Section 4 presents the impact of these land cover-driven changes on the tropospheric ozone burden in the midnineteenth century and the associated impact on the radiative forcing. Finally, conclusions are presented in section 5.

2. Model Description and Scenarios
2.1. The HadGEM2-ES Earth System Model
We use the global 3-D HadGEM2-ES model [*Collins et al.*, 2011] to simulate atmospheric chemistry, climate, and land surface for the midnineteenth century period and for the present day. The model has a horizontal resolution of 1.9° by 1.3°, with 38 hybrid height levels which extend from the surface up to an altitude of approximately 39 km. The model is run in free-running atmosphere mode, with prescribed sea surface temperatures, and radiation forced by off-line fields of greenhouse gas and aerosol concentrations. An explicit simulation of the land surface is included from the Met Office Surface Exchange Scheme (MOSES) II scheme [*Essery et al.*, 2003], including vegetation photosynthesis and stomatal conductance, driven by model climate and ambient CO_2, which directly affects dry deposition and biogenic emissions. The effects of simulated atmospheric concentrations of ozone and aerosol on the climate via interactions with the model radiation scheme or carbon cycle are not included.

The extended chemistry version of the UK Community Chemistry and Aerosol scheme is used to simulate atmospheric composition, featuring approximately 200 chemical reactions and accounting for 83 species. The scheme includes tropospheric CH_4-NO_x-CO-O_3 chemistry [*O'Connor et al.*, 2014] with the addition of simplified isoprene reactions [*Folberth et al.*, 2006; *Pacifico et al.*, 2015] based on the Mainz Isoprene Mechanism (MIM) [*Poschl et al.*, 2000]. In this study an updated version of the MIM was utilized where the rate coefficients of nitrogen-containing organic compounds were improved (M. Jenkin, unpublished data, 2012) based on the latest release of the Leeds master chemical mechanism (MCM: https://mcm.leeds.ac.uk/MCM/). This version of the MIM was recently used by *Pacifico et al.* [2015] to simulate the impacts of biomass burning-induced ozone damage on vegetation in the Amazon rain forest and was shown to perform well compared to observations over the region. This demonstrates that the updated MIM performs well under low NO_x-high isoprene conditions and is suitable to model the impacts of changing atmospheric chemistry-vegetation interactions in the midnineteenth century.

For the treatment of dry deposition of gas phase species and aerosols, a big leaf model approach is used as described by *Sanderson et al.* [2006], which uses stomatal conductance and LAI from the model vegetation scheme. Biogenic emissions of isoprene, a lumped monoterpene species, acetone, and methanol are calculated online using the interactive emissions scheme. The isoprene emissions scheme, as described by *Pacifico et al.* [2011], calculates the rate of isoprene synthase and emission based upon vegetation type and the rate of photosynthesis and dark respiration from the MOSES simulation. The CO_2 inhibition effect on isoprene emissions is accounted for using an empirical-based relationship derived from *Arneth et al.* [2007], which is dependent on the internal CO_2 concentration of the leaf and also includes the short-term response of emissions to drought stress [*Arneth et al.*, 2007]. Finally, emissions of NO_x from lightning are determined

interactively according to *Price and Rind* [1993]. Anthropogenic surface emissions are taken from the historical (1850 to 2000) gridded emissions dataset used for the Climate Model Intercomparison Program #5 (CMIP5) simulations [*Lamarque et al.*, 2010].

2.2. Prescribed Model Vegetation

For all of the simulations, model land cover is prescribed from a data set representative of historical changes in land use for the period 1750–2010, as produced for CMIP5 [*Hurtt et al.*, 2011]. These data are derived from the present-day climatology International Geosphere-Biosphere Programme (IGBP) data set [*Loveland et al.*, 2000] and reconstructions of anthropogenic land use from the History Database of the Global Environment (HYDE)3 data set [*Klein Goldewijk et al.*, 2010]. Each model gridbox area is partitioned into fractional coverage of nine land surface types. These represent five plant functional types (PFTs), broadleaf tree, needleleaf tree, C3 Grasses, C4 Grasses, and shrubs, plus four other land categories, urban, water, desert/bare ground, and land ice/glacier. For each model simulation the land cover distribution is fixed and sets to update leaf phenology on a daily basis which determines the evolution of model LAI.

2.3. Model Scenarios

A midnineteenth century control run (PI_CTRL) was driven using sea surface temperatures (SSTs) and sea-ice fields which were representative of the period 1860–1870 and varied on a monthly basis. Anthropogenic surface emissions for the 1860s and greenhouse gas concentrations were held fixed at 1860s concentrations (286 ppmv for CO_2, 0.8 ppmv for CH_4, and 276 ppbv for N_2O *Jones et al.* [2011]). The model was spun up for a period of 9 months and then run for 10 years with the analysis performed on climatological averages over the last 8 years of the simulation. This relatively short spin-up period is possible as we prescribe the slow, long-term responses of the vegetation to changes in CO_2 (i.e., vegetation dynamics) rather than simulate them interactively. This is done through prescribed land cover from the HYDE3 and IGBP data sets which have explicitly accounted for both natural and anthropogenic influences on the global vegetation distribution since the 1860s. Furthermore, by using fixed SSTs and greenhouse gas concentrations, and disabling feedbacks from changes in atmospheric ozone and aerosol to the model radiation scheme, these climatological averages are sufficient to produce stable, robust tropospheric distributions of ozone and associated trace gases consistent with the driving climate and land cover conditions.

An additional set of two simulations was run in order to test separately the sensitivity of the modeled midnineteenth century tropospheric ozone distribution to changes in land cover and climate. As with the PI_CTRL run, both of these scenarios were run for 10 years with the analysis performed on climatological averages of the last 8 years of the simulation. For the first simulation (VEG_2000), the prescribed model vegetation distribution was changed to be representative of the year 2000. This allowed the impacts of midnineteenth century to present-day vegetation changes on dry deposition and BVOC emissions to be simulated. The second simulation assessed the sensitivity of midnineteenth century tropospheric ozone to both changes in vegetation processes and model climate. For this simulation (CLIM_2000) the model was set up to simulate a present-day climate with fixed greenhouse gases and vegetation representative of the year 2000 (see Table 1). SSTs and sea-ice fields were also representative of the year 2000 and are prescribed as climatological monthly means for this simulation. For the CLIM_2000 simulation, the atmospheric chemistry scheme was driven using CH_4 representative of the midnineteenth century period (1860s). Anthropogenic surface emissions for the 1860s were retained. The setup of this CLIM_2000 scenario is equivalent to some previous model studies investigating pre-industrial ozone in chemical transport models using prescribed off-line meteorology for present day [*Hauglustaine and Brasseur*, 2001; *Lamarque et al.*, 2005; *Mickley et al.*, 2001]. For each of these additional scenarios, the model was also run for 10 years with the analysis performed on climatological averages over the last 8 years of the simulation.

Two further simulations were run to assess the sensitivity of ozone concentrations to variations in the prescribed CO_2 mixing ratio that is specified for the model vegetation scheme (CO_{2Veg}). For these simulations, the model is modified such that CO_{2Veg} only impacts the model vegetation trace gas exchange and affects only the simulated dry deposition and isoprene emissions. The standard CO_2 greenhouse gas concentration specified for the model climate simulation is specified separately and feeds through the rest of the model, including the carbon cycle. Furthermore, the CO_{2Veg} can be set to affect either dry deposition or isoprene emissions in isolation or both together. The change in CO_{2Veg} does not feedback to photosynthesis and therefore CO_2 fertilization of LAI is not affected in these scenarios. For the CO2_DD simulation, a CO_{2Veg} mixing ratio of 368 ppmv (representative of the year 2000) was specified, with the effects of this higher CO_{2Veg} being limited

Table 1. Summary of HadGEM2-ES Midnineteenth Century Model Scenarios to Assess Sensitivity of Midnineteenth Century Ozone to 1865 to 2000 Land Cover Change[a]

Model Scenario	Land Cover (LC)	Atmospheric CO_2	SST + Sea Ice	Chemistry and Aerosol Emissions[a]
PI_CTRL	1865	286 ppmv (all of model)	1860s	1860s
VEG_2000	2000	286 ppmv (all of model)	1860s	1860s
CO2_DD	1865	368 ppmv (dry dep only)	1860s	1860s
CO2_DDBVOC	1865	368 ppmv (iBVOC + dry dep only)	1860s	1860s
CLIM_2000	2000	368 ppmv (all of model)	2000s	1860s
PD_2000	2000	368 ppmv (all of model)	2000s	2000s

[a]Surface-emitted species include the following: NO_x, CH_4, CO, HCHO, C_2H_6, C_3H_8, Me_2CO, MeCHO, APIN, NVOC, MEK, C_4H_{10}, AROM, C_2H_4, and C_3H_6.

to the dry deposition (through stomatal uptake) of atmospheric trace species only. For the CO2_DDBVOC simulation, the CO_{2Veg} mixing ratio of 368 ppmv impacts both the stomatal uptake of trace species and also the emission of BVOCs through the land model iBVOC scheme. For both of these simulations the impacts of higher CO_{2Veg} concentrations affect the chemistry only and do not feedback on the model climate through impacts on the carbon cycle and water transpiration, with the rest of the model processes forced by a standard midnineteenth century concentration of 286 ppmv. The CO2_DD and CO2_DDBVOC simulations are spun up for a period of 9 months and then run for 3 years with the analysis performed on the final year of each run. In order to assess the impact of changing CO_{2Veg} on ozone concentrations, we compared with the corresponding year from the PI_CTRL for comparison. Shorter simulations are sufficient in these cases, since the simulated changes in dry deposition and biogenic emissions only impact the simulated chemical composition of the atmosphere, which does not feed back to the model radiation scheme and dynamics. These additional scenarios are summarized in Table 1.

The main aim of this study is to highlight the sensitivity of the simulated midnineteenth century tropospheric ozone distribution to the model prescribed vegetation cover and assumed atmospheric chemistry-vegetation interactions (namely the effect of CO_2 on dry deposition and isoprene emissions). Therefore in order to explicitly isolate the responses of these changes and to estimate the model response in a midnineteenth century atmosphere we fix anthropogenic emissions at values representative of the 1860s. Figures 1a, 1c and 1e show anthropogenic NO_x emissions for 1865 where global annual emissions are estimated at 34.3 Tg NO_x yr^{-1}. As shown in Figures 1b, 1d, and 1f show that emissions of NO_x are considerably larger in 2000, with global annual emissions a factor of 4 larger at 138.1 Tg NO_x yr^{-1}), with the largest increases seen over the major industrialized regions of North America, Europe and SE Asia. Holding emissions fixed at 1865 levels ensures that the differences between simulations are due to atmospheric-chemistry vegetation interactions rather than changes in the NO_x regime.

Finally, a near present-day (PD_2000) scenario was simulated to evaluate 1865 to 2000 changes in the tropospheric ozone burden and resultant radiative forcing. For this simulation, the model used climatological monthly mean sea surface temperatures (SSTs) and sea ice fields representative of the 2000s. Anthropogenic surface emissions were prescribed from CMIP5 and were set at levels representative of 2000s and greenhouse gases were held fixed at 2000s concentrations [368 ppmv for CO_2, 1.7 ppmv for CH_4 and 330 ppbv for N_2O [*Jones et al.*, 2011]]. A summary of the PD_2000 is shown in Table 1.

2.4. 1865 to 2000 Land Cover Changes
Table 2 shows changes in global and regional distributions of the five model vegetation plant functional types (PFTs) between 1865 and 2000. The broadleaf tree, needleleaf tree, and shrub categories show a decline in global coverage with shrubs showing the largest decline (1404.1 Mha or −54.0%) and needleleaf trees showing the smallest (218.5 Mha or −15.7%). Both C3 and C4 grasses (which included agricultural crops and pastureland) show increases in global coverage of 1736.9 Mha (105.1%) and 933.0 Mha (152.9%), respectively. This reflects the general change in land patterns from the midnineteenth century to the present day due to anthropogenic activity resulting in the replacement of forested regions by agricultural crops since the 1850s [*Ramankutty and Foley*, 1999; *Richards*, 1990; *Turner et al.*, 1993]. On a regional scale, changes in coverage of needleleaf tree (−150.7 Mha or −13.3%), C3 grass (847.3 Mha or +134.7%), and shrubs (−726.1 Mha or −59.8%) are most pronounced over the Northern Hemisphere midlatitude regions, with changes for broadleaf trees
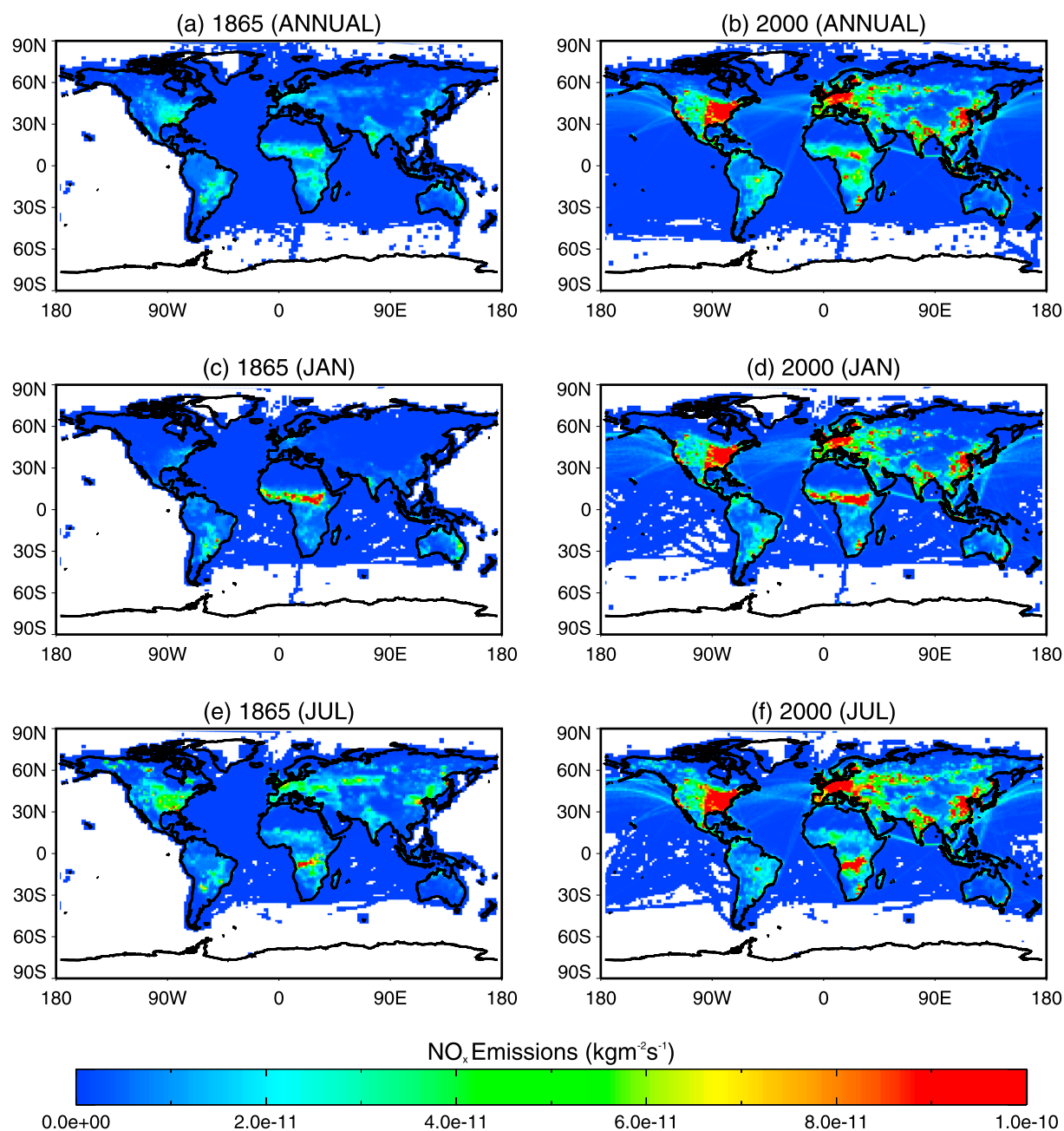
Figure 1. (a, b) Global mean annual NO$_x$ emissions for the 1860s under the PI_CTRL scenario. Monthly mean NO$_x$ emissions are shown for (c, d) January and (e, f) July to highlight the seasonality in emissions.

and C4 grasses largest over the tropics (−721.9 Mha (−24.3%) and 548.4 Mha (+159.6%), respectively). This change in broadleaf tree coverage over the tropics is of particular relevance, due to their role as large emitters of isoprene in the tropics [*Guenther et al.*, 2006].

2.5. Calculation of Tropospheric Ozone Radiative Forcing

We use the off-line version of the *Edwards and Slingo* [1996] radiative transfer model to calculate the radiative effects of our simulated changes in tropospheric ozone [*Rap et al.*, 2015]. This model uses six bands in the shortwave, nine bands in the long wave and a delta-Eddington 2 stream scattering solver at all wavelengths. The code uses monthly averaged climatology of temperature, water vapor, and trace gases based upon the European Centre for Medium-Range Weather Forecasts reanalysis data. The resolution is 2.5°×2.5° in the horizontal with 23 pressure levels in the vertical from the surface up to 1 hPa [*Rap et al.*, 2015]. Cloud and surface

Table 2. Global and Regional Differences in HadGEM2-ES PFT Coverage in Mha Between 1865 and 2000

PFT	Globe	Tropics	NH Midlatitude	SH Midlatitude
Broadleaf tree	−1092.4 Mha	−721.9 Mha	−230.2 Mha	−140.9
Needleaf tree	−218.5 Mha	−46.4 Mha	−150.7 Mha	−24.0
C3 grass	1736.9 Mha	636.9 Mha	847.3 Mha	257.7
C4 grass	933.0 Mha	548.4 Mha	228.5 Mha	156.8
Shrubs	−1404.1 Mha	−428.3 Mha	−726.1 Mha	−252.2

albedo data are compiled from the International Satellite Cloud Climatology Project archive [*Rossow and Schiffer*, 1999] and averaged over the time period 1983 to 2008. The calculated radiative forcing is the stratospherically adjusted radiative forcing defined as the change in net irradiance at the tropopause after allowing for the readjustment of stratospheric temperatures to radiative equilibrium while holding surface and tropospheric temperature and state variables (e.g., water vapor and cloud cover) fixed at the unperturbed values [*Myhre et al.*, 2013]. For the purpose of the off-line radiative calculations only, stratospheric ozone (here we use the chemical tropopause definition based upon the 150 ppbv ozone concentration) is kept constant at present-day concentrations for each scenario during the radiative calculations, in order to isolate the radiative response to tropospheric ozone changes only.

3. Results and Discussion

3.1. Sensitivity of Atmospheric Chemistry-Vegetation Interactions to Land Cover and CO_2 Changes

A number of key interactions dominate the expected response of atmospheric composition to changes in vegetation processes (Figure 2). Key effects are the response of dry deposition and isoprene emissions to vegetation cover changes and the impact of changing CO_2 on these processes. Land use change from the
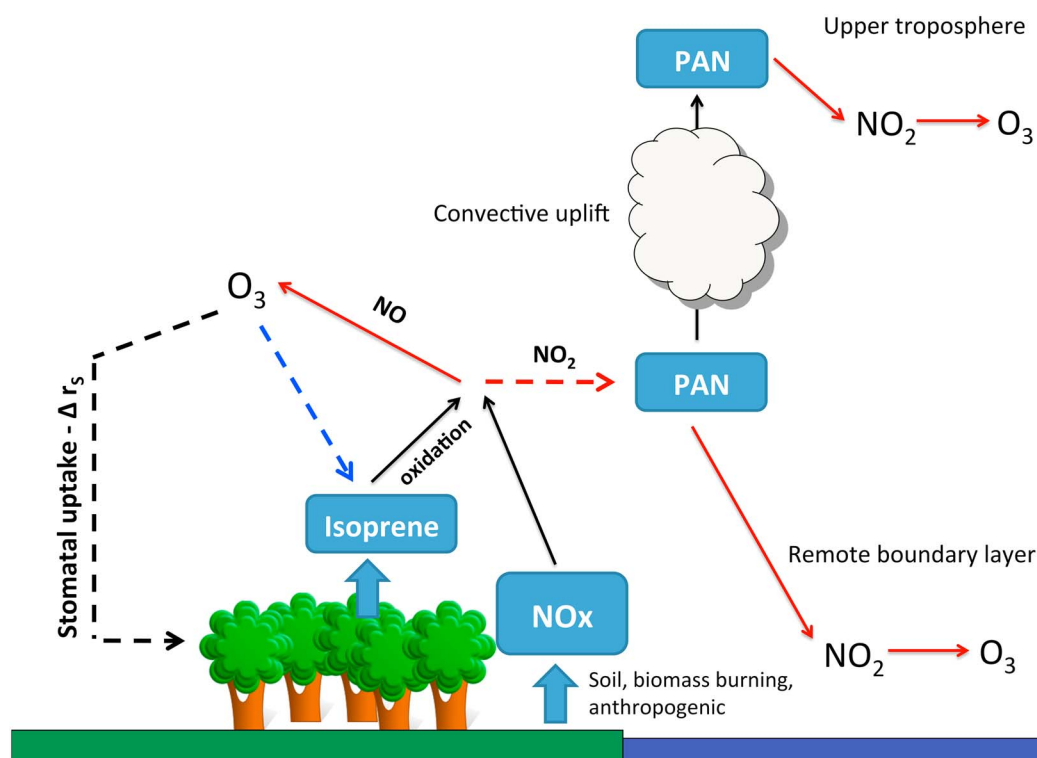

Figure 2. Chemical processes resulting from vegetation land cover change that impact tropospheric ozone. Blue arrows indicate processes dominant in low NO_x conditions, while red arrows are dominant in the presence of elevated NO_x. Dashed arrows show reactions or conversions that suppress ozone formation, while solid arrows enhance ozone formation. The formation of PAN from the reaction of NO_2 with isoprene oxidation products is a key pathway between changes in surface vegetation and ozone production and loss locally, over the remote marine regions and in the upper troposphere, where PAN can be transported in deep convection and frontal uplift.
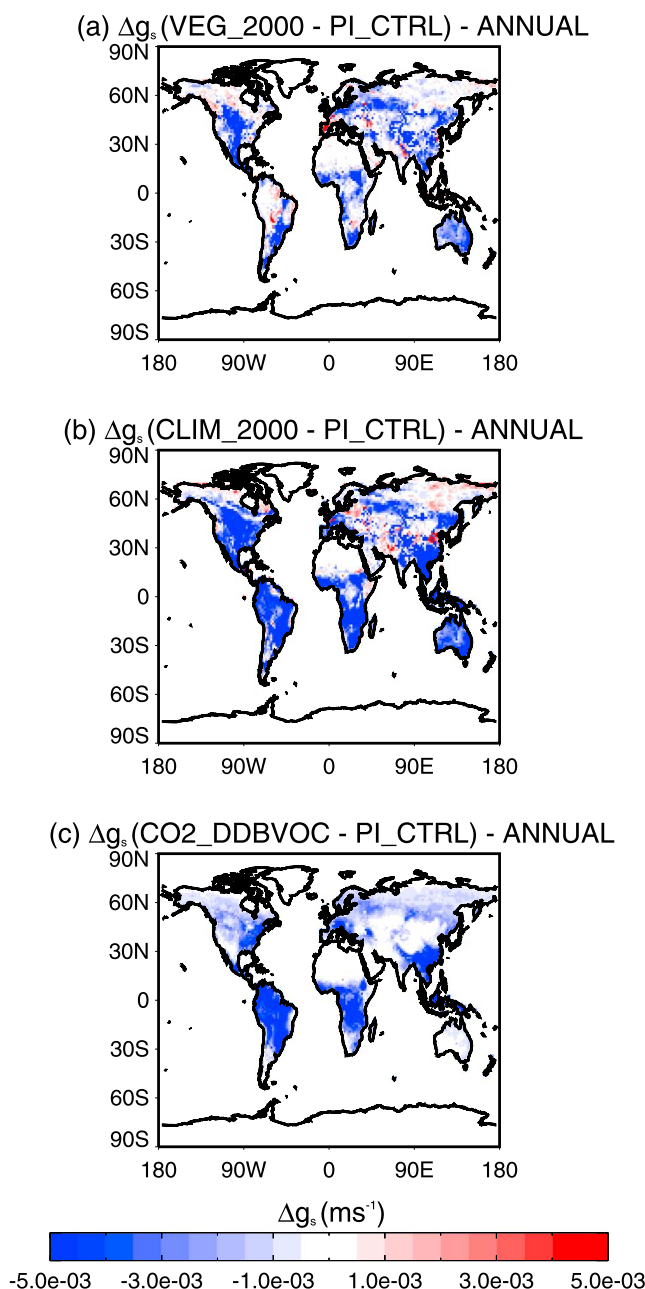
Figure 3. Changes in annual mean stomatal conductance (m s^{-1}) under the VEG_2000, CLIM_2000, and CO2_DDBVOC scenarios with respect to the PI_CTRL simulation. Note that stomatal conductances are total gridbox stomatal conductance over all PFT types.

midnineteenth century to the near present day involved the reduction in forest area and a replacement with large areas of cropland [*Ramankutty and Foley*, 1999; *Richards*, 1990]. This acted to reduce the rate of dry deposition [*Ganzeveld and Lelieveld*, 1995] of ozone and its precursors to the land surface and thus results in a local rise in concentrations. Further to this cropland species tend to emit lower amounts of isoprene which further contributes to a local increase in ozone concentrations, through a reduction in isoprene ozonolysis, and also acts to limit PAN formation. This can reduce the long-range transport of reactive nitrogen and thus lead to a drop in remote ozone concentrations away from the high-isoprene sources. Further to this is the effect of changing CO_2 concentrations which can reduce the rate of dry deposition by inducing stomatal closure. Finally, as discussed previously, higher CO_2 can also contribute to reduced isoprene emissions due to the inhibition effect. The key determinants in how changes in isoprene emissions affect ozone both locally and in

the remote troposphere are the presence or absence of NO_x and the role of isoprene as a precursor for PAN formation. We discuss how these pathways are affected under each of our scenarios below.

3.1.1. Impact of Vegetation and CO_2 Changes on Stomatal Trace Gas Uptake

Figure 3 shows the changes in annual mean stomatal conductance between each of the four model scenarios and the control simulation (PI_CTRL). Under the VEG_2000 scenario (Figure 3a), stomatal conductances are lower in general than under the PI_CTRL scenario by around 5.0×10^{-3} ms^{-1} (~20%), with a few locations seeing changes as large as 10.0×10^{-2} ms^{-1} (~100%). These largest differences are simulated over the Northern Hemisphere developed regions of North America, Europe, and Southeast Asia, along with some tropical regions, and reflect locations of replacement of forests with crops and grasses (Table 2). The associated reduction in mean stomatal conductance in these regions is due to lower LAI and conductance rates over crop and grasslands compared to forested regions [*Ganzeveld and Lelieveld*, 1995].

Under the CO2_DDBVOC scenario (Figure 3c) the model vegetation is exposed to a higher fixed present-day CO_2 mixing ratio of 368 ppmv compared to the lower midnineteenth century mixing ratio of 286 ppmv under the PI_CTRL scenario, resulting in the same reductions in stomatal conductance under both scenarios. This response is consistent with higher CO_2 mixing ratios inducing stomatal closure in vegetation [*Gedney et al.*, 2006]. The largest differences are simulated over the tropical rain forest regions where stomatal conductances are up to 5.0×10^{-3} ms^{-1} (~20%) lower than under the PI_CTRL scenario. This largely reflects the geographical distribution of broadleaf tree species. However, widespread regions of North America, Southeast Asia, and Europe see significant drops in stomatal conductance of up to 2.0×10^{-3} ms^{-1} (around 12%) under higher CO_{2Veg}. This reduction in stomatal conductance results in an overall reduction in the rate of dry deposition uptake of trace species under both scenarios when compared to the PI_CTRL scenario.

Under the CLIM_2000 scenario (Figure 3b) the response of stomatal conductances reflects both the changes in land use under the VEG_2000 scenario and the elevated CO_{2Veg} under the CO2_DDBVOC scenario. The large-scale replacement of forests with cropland is evident over the northern hemisphere developed regions and the effect of the elevated CO_{2Veg} on reducing stomatal conductance is evident over the tropical rain forest regions. However, reductions in stomatal conductance are more widespread than seen under the VEG_2000 and CO2_DDBVOC scenarios with more regions showing reductions of 5.0×10^{-3} (20%), with a few locations seeing changes as high as 10.0×10^{-2} ms^{-1} (~100%) (e.g., over the Amazon rain forest).

3.1.2. Impact of Vegetation and CO_2 Changes on Isoprene Emissions

Figure 4 shows the changes in annual mean isoprene emissions under the VEG_2000, CO2_DDBVOC, and CLIM_2000 scenarios relative to the PI_CTRL scenario. Emissions for the CO2_DD scenario are the same as those under the PI_CTRL scenario, since the higher CO_2 mixing ratio in this simulation only impacts dry deposition.

The replacement of high isoprene emitting broadleaf trees with grasses and crops under the VEG_2000 scenario leads to a reduction of 109 Tg C yr^{-1} in isoprene emissions compared with the PI_CTRL scenario emissions of 580 Tg C yr^{-1}. Geographically, largest differences are in regions where broadleaf trees are replaced with crops and grasses, over the Northern Hemisphere developed regions and the tropics (Table 2). This reduction is consistent with but slightly lower than the 1850–2000 land use change-induced reduction in isoprene emissions of 135 Tg C yr^{-1} estimated by *Unger* [2014].

As discussed in previous studies [*Heald et al.*, 2009; *Pacifico et al.*, 2009; *Young et al.*, 2009; *Pacifico et al.*, 2012], higher CO_2 mixing ratios can result in the inhibition of isoprene emissions from vegetation. This is accounted for in the model photosynthesis-driven iBVOC scheme (See section 2.1) and results in isoprene emissions of 456 Tg C yr^{-1} in the CO2_DDBVOC simulation, compared to 580 Tg C yr^{-1} in the PI_CTRL scenario. Largest differences in isoprene emissions due to the higher CO_{2Veg} are simulated over the tropical broadleaf forested regions where widespread regions show reductions in isoprene emissions of 1.0×10^{-10} kg C m^{-2} s^{-1} (~19%), with maximum reductions of 2.8×10^{-9} kg C m^{-2} s^{-1} (~22%) seen over the Amazon rain forest. Large reductions are also seen over widespread parts of North America, Southeast Asia, and Europe where isoprene emissions are lower in the CO2_DDBVOC scenario by up to 4.0×10^{-11} kg C m^{-2} s^{-1} (~20%). The reduction of -124 Tg C yr^{-1} in global isoprene emissions relative to the PI_CTRL simulation is slightly larger than that produced by the VEG_2000 scenario (-109 Tg C yr^{-1}). The magnitude of this change is in agreement with the findings of *Pacifico et al.* [2012] who reported a similar magnitude response (133 Tg C yr^{-1}) using the same iBVOC scheme with present day and midnineteenth century CO_2 mixing ratios. Under the CLIM_2000 scenario the reductions in isoprene emissions follow a similar pattern to those under the VEG_2000 scenario but are more pronounced. This is due to the combination of the effects of vegetation change and CO_2 inhibition.
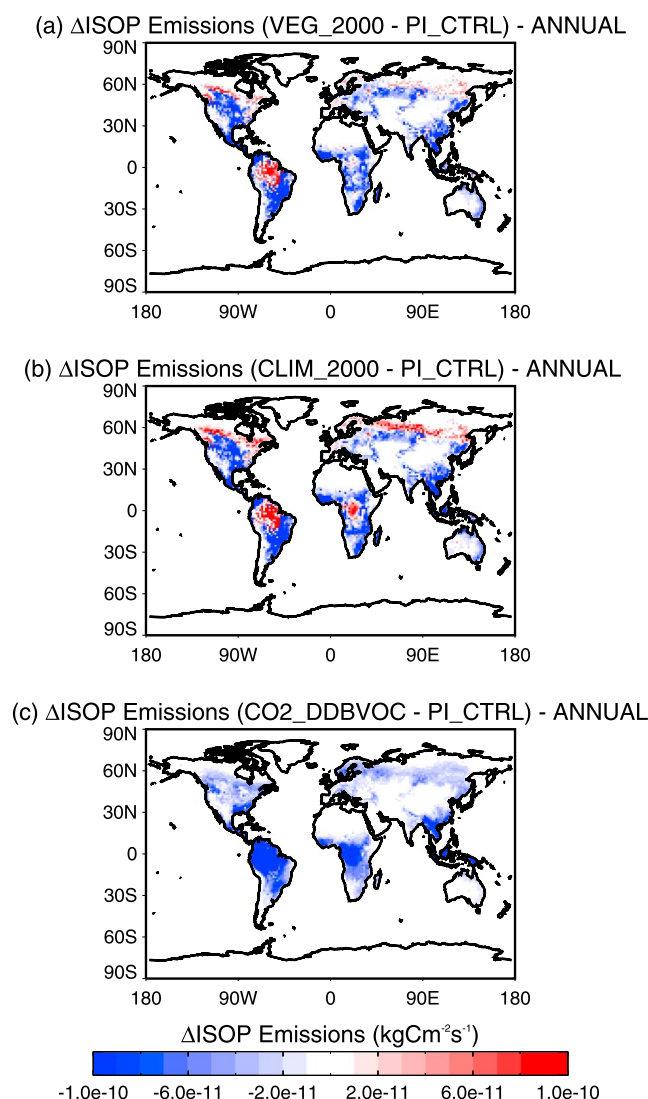
Figure 4. Changes in annual mean isoprene emissions (kg C m^{-2} s^{-1}) under the VEG_2000, CLIM_2000, and CO2_DDBVOC scenarios with respect to the PI_CTRL simulation.

It should be noted that large uncertainties exist in the CO_2 inhibition effect on isoprene emissions at the subambient CO_2 concentrations of the nineteenth century. It has been shown in previous studies using limited plant species that increasing CO_2 from a subambient baseline (e.g., 240 ppmv) to present-day concentrations (around 380–400 ppmv) produces mixed responses dependant on plant species [*Wilkinson et al.*, 2009; *Possell et al.*, 2005]. This will thus introduce uncertainties in the responses of isoprene emissions to the change in CO_2 simulated in this study for 1865. However, despite these mixed responses and limited data for subambient CO_2, a consistent picture is emerging that rise in CO_2 since the midnineteenth century in general leads to a decrease in the isoprene emission rate [*Possell et al.*, 2005; *Wilkinson et al.*, 2009].

The effect of CO_2 inhibition and land cover-induced changes in isoprene emissions on tropospheric ozone is sensitive to the magnitude and distribution of emissions of NO_x. Under conditions of low NO_x abundance, isoprene may act as a net sink for tropospheric ozone [*Barket et al.*, 2004; *Pacifico et al.*, 2009]. This occurs where the direct reaction of ozone with isoprene becomes competitive with ozone production resulting from reaction of NO with peroxy radicals produced during isoprene oxidation. Global surface emissions of NO_x in our 1865 simulations are approximately a factor 4 lower than in present day (34.3 Tg NO_x yr^{-1} compared to 138.1 Tg NO_x yr^{-1})). The result is that many regions in which an increase in isoprene results in net ozone production in present day, instead see a net ozone loss. We discuss these effects further in the following section.
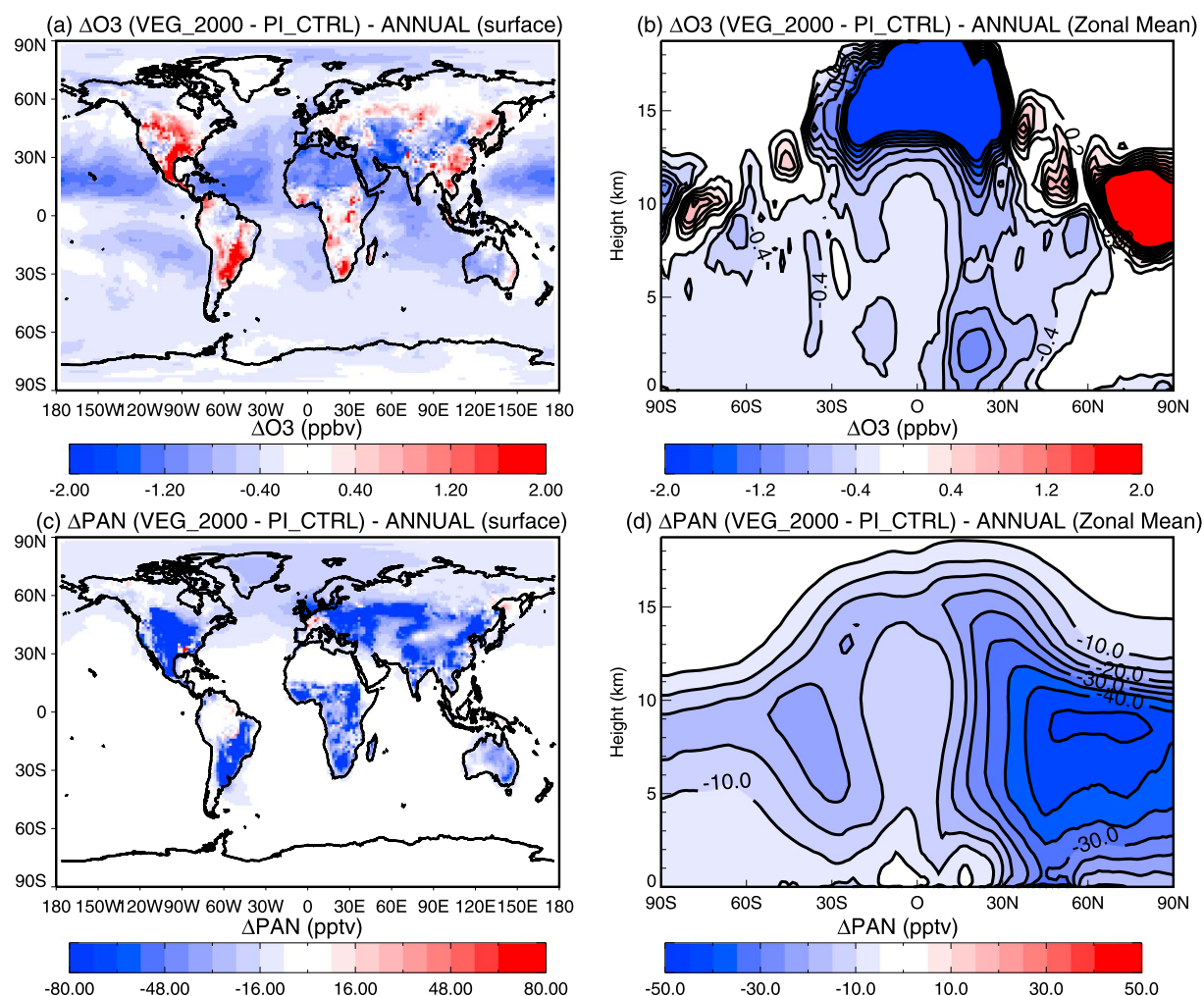
Figure 5. Changes in (a) annual mean surface ozone , (b) annual mean zonal mean ozone, (c) annual mean surface PAN, and (d) annual mean zonal mean PAN under the VEG_2000 scenario with respect to the PI_CTRL simulation.

3.2. Sensitivity of Midnineteenth Century Tropospheric Composition to Vegetation and CO_2 Changes

3.2.1. The 1865 to 2000 Vegetation Change VEG_2000 VS. PI_CTRL

Figure 5 shows the response of annual mean surface and annual zonal mean ozone and PAN concentrations to land cover change between 1865 and 2000, under midnineteenth century surface emissions and climate. Surface ozone concentrations under the VEG_2000 simulation are up to 2 ppbv greater over parts of North America, Southeast Asia, South America, and Africa compared to the midnineteenth century control scenario, corresponding to regions of greatest loss of tree cover and replacement with grass-type vegetation (Table 2). This increase in surface ozone can be attributed to two different influences. First, a reduction in stomatal conductance over these locations (Figure 3) leads to a reduction in the rate of dry deposition of ozone and its precursor species (e.g., NO_2 and PAN) to the land surface. This results in an increase in surface ozone concentrations. Second, the transition from broadleaf tree PFT type to grasses leads to a reduction in isoprene emissions which acts to further increase surface ozone concentrations. This is because despite the reduction in isoprene emissions, the reduction in PAN formation leads to elevated local NO_x concentrations which in turn drives increased ozone formation. Furthermore, the reduction in isoprene emissions in the overall low NO_x 1865 environment reduces the direct reaction between ozone and isoprene further contributing to higher ozone concentrations.

In contrast, away from isoprene source regions, ozone concentrations under the VEG_2000 scenario are lower than under the PI_CTRL simulation by up to 1.5 ppbv (e.g., northern Africa, central Asia, and Australia). Lower concentrations are also simulated over the oceans of at least 0.4 ppbv, with reductions of up to 2 ppbv over
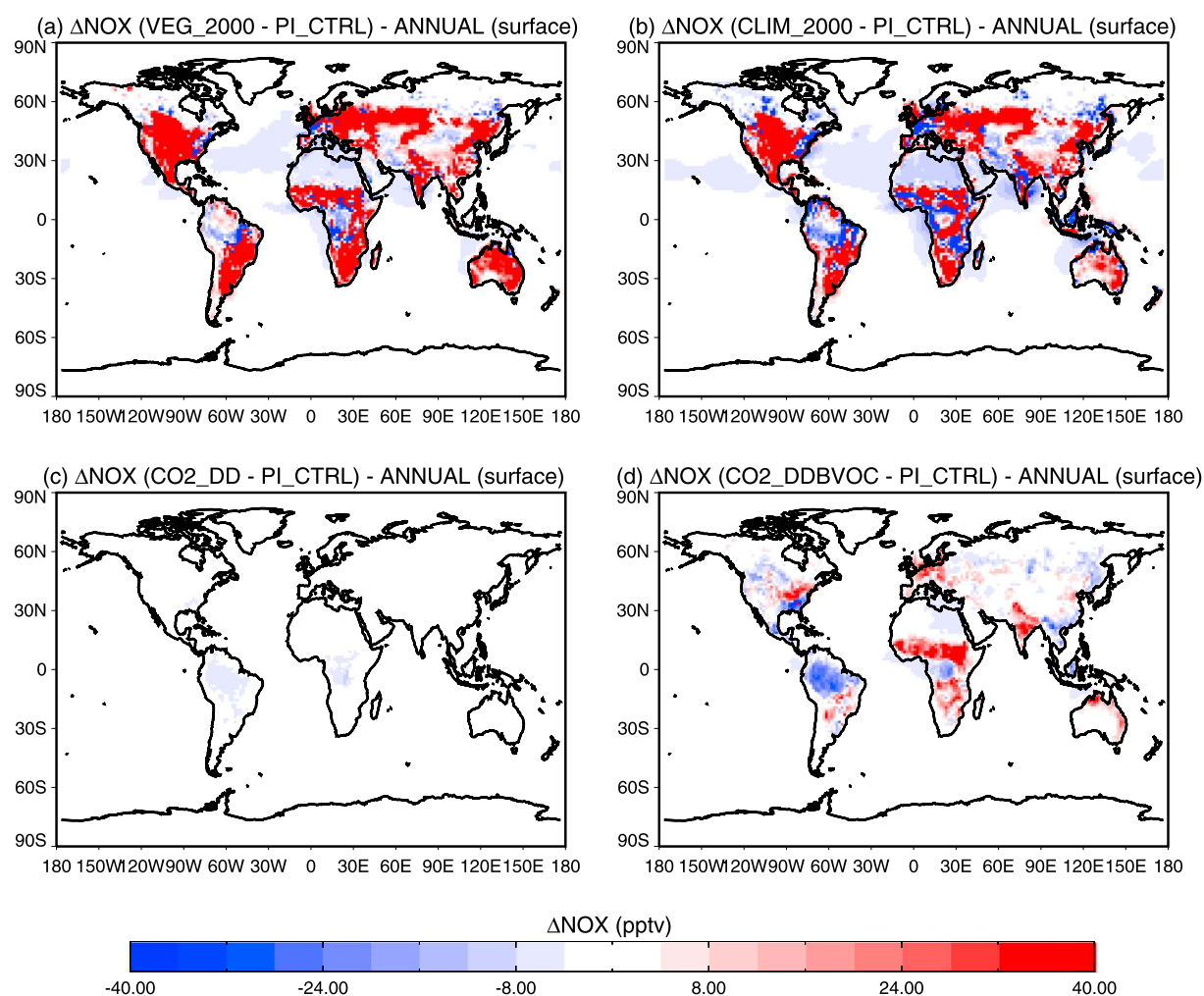
Figure 6. Changes in annual mean surface NO_x (pptv) under the VEG_2000, CLIM_2000, CO2_DD, and CO2_DDBVOC scenarios with respect to the PI_CTRL simulation.

the tropical oceans. Under the VEG_2000 scenario, PAN mixing ratios are reduced compared with those in the PI_CTRL scenario by 50 pptv or greater over large parts of the continental land masses. As reductions in isoprene emissions over the Northern Hemisphere and tropical continents (Figure 4) are colocated with areas of greatest surface midnineteenth century NO_x emissions (Figure 1), lower isoprene results in a substantial reduction in formation of PAN. This reduction in PAN formation in the VEG_2000 simulation leads to reduced transport of reactive nitrogen to the remote marine locations and a consequent reduction in remote tropospheric ozone formation. This effect is evident in Figure 6 where surface NO_x concentrations are lower under the VEG_2000 scenario by at least 10 pptv with mixing ratio reductions of up to 20 pptv over the tropical marine regions. Over the continents, NO_x mixing ratios are higher under the VEG_2000 scenario by values of 50 pptv or higher in correspondence to the regions where the effects of reduced dry deposition lead to a net local increase in NO_x. This also contributes to the higher ozone values seen in these regions under the VEG_2000 scenario.

The impact of the lower isoprene emissions under the VEG_2000 scenario on free tropospheric ozone is evident in Figure 5. Modeled ozone concentrations are generally lower than under the PI_CTRL scenario by 0.4 ppbv to 0.8 ppbv throughout the free troposphere. Larger differences of around 1 ppbv are seen near the surface through the Northern Hemisphere tropics, and reductions in ozone concentrations of 2–6 ppbv are simulated in the upper troposphere lower stratosphere region over the tropics of both hemispheres. These ozone reductions also result from reductions in PAN transport into the free troposphere under the VEG_2000 scenario. PAN concentrations are homogeneously lower throughout the entire troposphere by at least 4 pptv
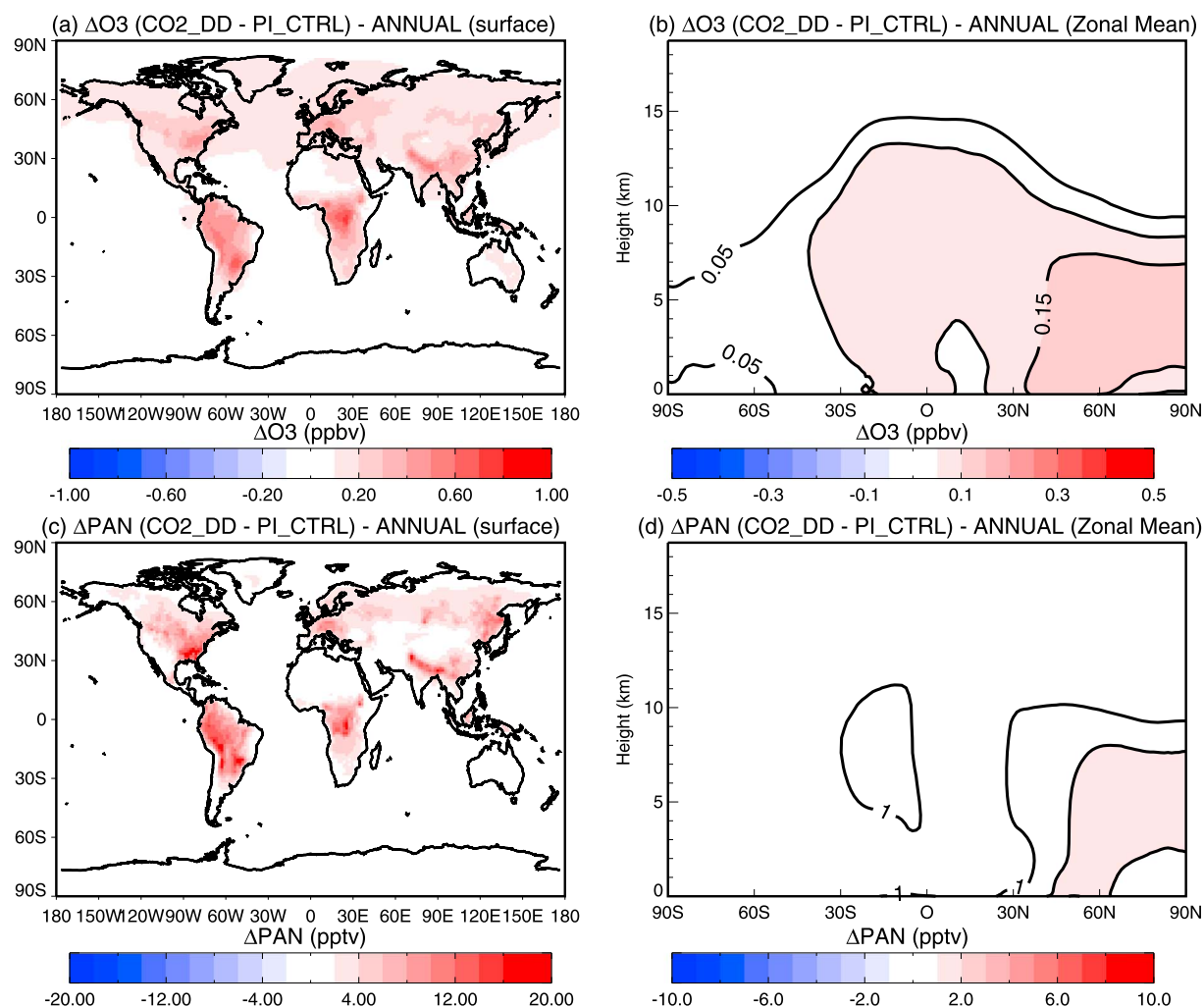
Figure 7. As in Figure 5 except for the CO2_DD versus PI_CTRL scenarios.

(10%) with the largest differences seen in the Northern Hemisphere free troposphere where concentrations are up to 50 pptv lower (20%, Figure 5d). The extent of the ozone and PAN reductions in the upper Northern Hemisphere free troposphere, particularly over the tropics, highlight the importance of efficient vertical transport in this region due to deep tropical convection (see schematic Figure 2). As shown in sections 3.2.2 and 3.2.3, changes in PAN concentrations (Figures 7d and 8d) demonstrate that isoprene emissions changes have the dominant impact on upper tropospheric PAN and ozone (more so than dry deposition changes). This supports our assertion that these changes in tropical isoprene have widespread impacts on reactive nitrogen and ozone in the free troposphere. Contributing to this are larger nonanthropogenic annual emissions of NO_x in the tropical regions (Figure 1) from sources including lightning, biomass burning, and soil emissions.

Once transported to the upper troposphere (UT), the PAN lifetime increases as it becomes stable in the cold UT temperatures, and it is transported poleward in the global Hadley circulation. Consequently, changes in the rate of PAN formation from isoprene emission changes in the tropics have impacts on reactive nitrogen abundances, and hence our simulated ozone, throughout the global free troposphere, particularly under the midnineteenth century emissions scenario, where other sources of PAN (e.g., from midlatitude anthropogenic emissions) are absent or substantially lower.

3.2.2. Ozone Sensitivity to CO_2 Impacts on Dry Deposition Only (CO2_DD Versus PI_CTRL)

Figure 7 shows the differences in annual mean ozone and PAN concentrations between the CO2_DD and PI_CTRL scenarios. Dry deposition is suppressed due to reduced stomatal conductance under a higher CO_2 mixing ratio in the CO2_DD simulation. Consequently, ozone concentrations increase compared to those in
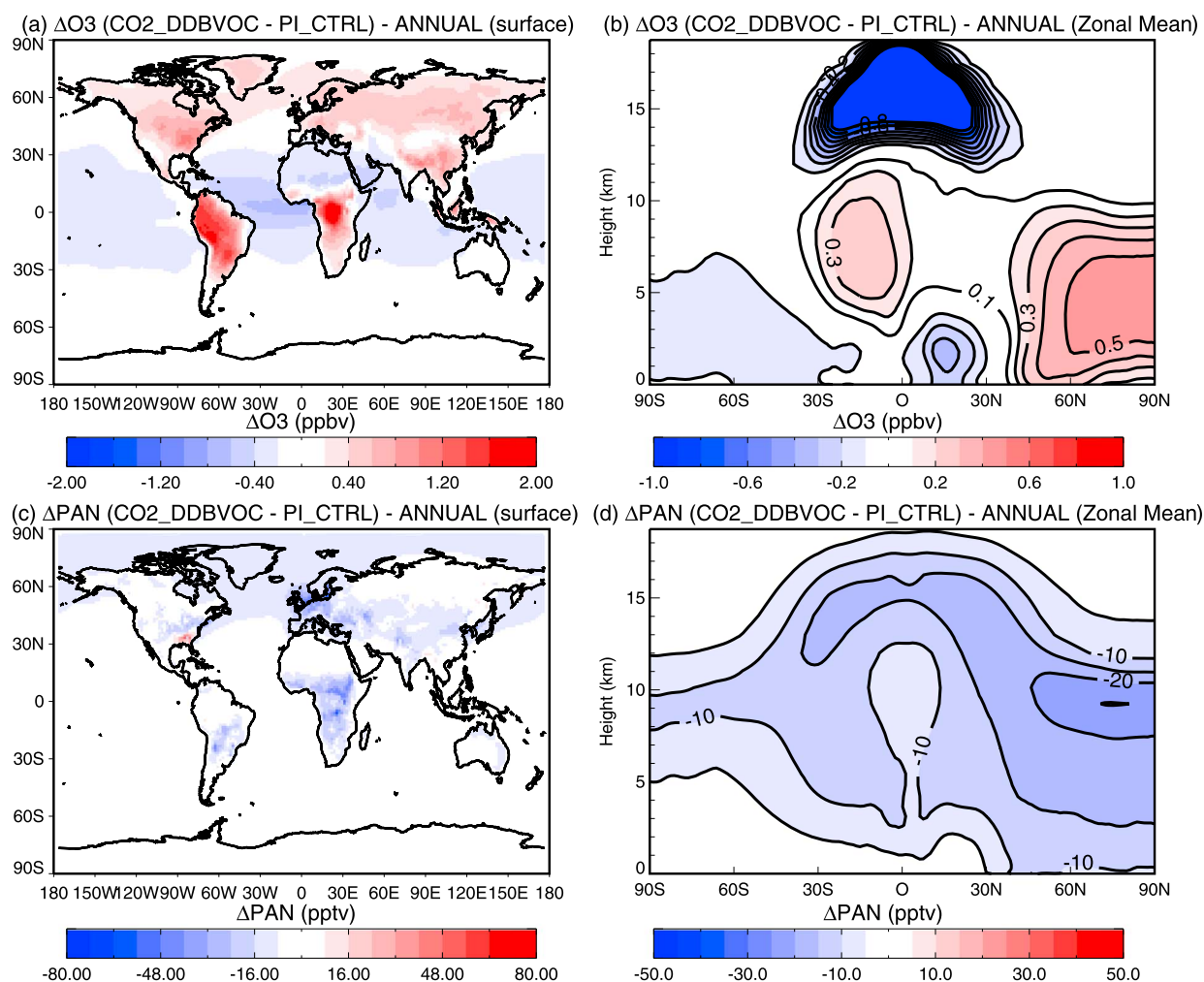
Figure 8. As in Figure 5 except for the CO2_DDBVOC versus PI_CTRL scenarios.

the PI_CTRL scenario. In the Southern Hemisphere, largest differences are simulated over the Amazon and central parts of Africa, where ozone concentrations are up to 1 ppbv greater than under the PI_CTRL scenario. This effect is due to the high coverage of broadleaf trees and high rates of photosynthesis, resulting in a strong response of stomatal conductance (Figure 3c). Surface ozone concentrations are greater by at least 0.2 ppbv throughout the majority of the Northern Hemisphere and up to 1 ppbv over eastern parts of the United States, Europe, and southeastern parts of Asia. The lower rates of ozone deposition lead to homogeneously higher ozone concentrations throughout the free troposphere under the CO2_DD scenario by at least 0.1 ppbv.

Dry deposition is also an important sink for PAN and NO_2, leading to enhanced PAN mixing ratios under the CO2_DD scenario. Largest differences are simulated over the Amazon and central Africa in the Southern Hemisphere (10–20 pptv) and over widespread regions of North America, Europe, and eastern Siberia in the Northern Hemisphere where differences are 20 pptv or larger, with consequent impacts on remote tropospheric ozone, as discussed in the previous section. As a result of these higher PAN mixing ratios, more NO_x is locked up as PAN, resulting in slightly lower NO_x mixing ratios under the CO2_DD scenario with the greatest reductions of 10 pptv seen over South America and Central Africa (Figure 6).

3.2.3. Ozone Sensitivity to Combined CO_2 Impacts on Dry Deposition and Isoprene Emissions (CO2_DDBVOC Versus PI_CTRL)

The combined effects of reduced rates of dry deposition and isoprene emissions under the CO2_DDBVOC scenario compared with PI_CTRL are shown in Figure 8. These effects result in an almost universal increase in surface ozone concentrations over the NH and tropical continents. These increases in surface ozone show a similar spatial pattern to those simulated in the CO2_DD scenario, but are more pronounced in regions of

strong isoprene emission, and more widespread through the Northern Hemisphere. The CO_2 inhibition of isoprene emissions in the CO2_DDBVOC scenario acts to reduce isoprene emissions globally in all regions (Figure 4). The uniform increase in surface ozone in NH continental regions is consistent with isoprene acting as a net ozone sink in these regions under low midnineteenth century NO_x emissions, but it is also partly a response to less efficient dry deposition under enhanced CO_2 concentrations.

Surface ozone mixing ratios are lower under the CO2_DDBVOC scenario over the remote regions with differences approaching 1 ppbv over the tropical Atlantic. This response is similar to that shown in the VEG_2000 scenario and is a result of reduced PAN formation in tropical regions under reduced isoprene emissions. This leads to lower PAN and NO_2 abundances and ozone production rates over the remote marine regions. Figure 8 shows reductions in PAN mixing ratios under the CO2_DDBVOC scenario compared with PI_CTRL. Largest differences are simulated over parts of North America, Europe, South America, and central Africa where PAN concentrations are up to 40 pptv lower.

PAN reductions are smaller than those produced under the VEG_2000 scenario (Figure 5). This is because CO_2-induced reductions in dry deposition enhance PAN concentrations which subsequently partially offset the reduced PAN formation as a result of the lower isoprene emissions. Different spatial patterns and magnitudes of isoprene emission reductions produced by the change in vegetation compared to the change in global CO_2 mixing ratio (Figure 4) also play a role in these different responses. The response in surface NO_x concentrations (Figure 6d) shows a similar pattern to that from the VEG_2000 scenario; however, the increases in NO_x concentrations over the land masses are much less pronounced at around 30 pptv compared to 50 pptv or larger under the VEG_2000 scenario. Over the remote marine regions, NO_x concentrations are lower under the CO2_DDBVOC scenario than under the PI_CTRL scenario due to reduced PAN formation, as discussed above. These changes in NO_x have consequent impacts on surface ozone concentrations as discussed in section 3.2.1.

The more moderate reduction in PAN concentrations, than seen for the VEG_2000 scenario, also leads to contrasting zonal mean tropospheric ozone responses in each hemisphere. In the Southern Hemisphere, ozone reduces under the CO2_DDBVOC scenario by $0.1-0.2$ ppbv due to the PAN-induced reduction in ozone formation over the remote marine areas. In the Northern Hemisphere (NH), ozone increases at high latitudes and in the free troposphere. This is a consequence of the combined reductions in dry deposition and isoprene emissions under enhanced CO_2. Over the Northern Hemisphere continents, isoprene acts as an ozone sink, and the larger proportion of land mass in the northern hemisphere also results in a large reduction in dry deposition loss of ozone and its precursors. For this scenario in the NH, these effects dominate over the effects of a reduction in PAN due to lower isoprene emissions, which caused substantial free tropospheric ozone reductions in the VEG_2000 scenario.

3.2.4. Impacts of Model Climate (CLIM_2000 Versus PI_CTRL)

Tropospheric ozone mixing ratios are greater under the CLIM_2000 scenario by at least 2 ppbv throughout the Northern Hemisphere free troposphere compared with PI_CTRL. Largest differences of $6-8$ ppbv are simulated in the midlatitude upper troposphere (Figure 9). Ozone differences include the effects of both vegetation change and CO_2 increase on dry deposition and isoprene emissions, as well as the effects of the changes in SSTs, sea ice fields, and greenhouse gas concentrations between 1860 and 2000. These changes all combine to produce increases in surface ozone in the CLIM_2000 simulation over most of the Northern Hemisphere and tropical southern hemisphere continents, and ozone decreases over the remote SH oceans. Ozone increases are as much as 5 ppbv over parts of North America and the North Atlantic and at least 1 ppbv in most NH continental regions. In the tropics and Southern Hemisphere, ozone increases and decreases are colocated with isoprene emission reductions and increases, respectively (Figure 4), due to the ozone sink effect of isoprene under low NO_x.

The increases in NH continental surface ozone simulated in the CLIM_2000 simulation relative to the PI_CTRL scenario are more substantial than under any of the other scenarios. This is mainly due to the effects of the change in climate on stomatal conductance (Figure 3) producing substantial reductions in dry deposition velocities, compounding the effects of CO_2 increases, and land cover change over many regions. In addition climate impacts on circulation, atmospheric kinetics, and lightning emissions also contribute to these large ozone changes. Large differences in stratospheric ozone are simulated, since the CLIM_2000 simulation uses prescribed stratospheric ozone representative of the driving climate of year 2000, which is lower than that for a midnineteenth century atmosphere (PI_CTRL scenario).

The effects of climate change and isoprene emission reductions have substantial impacts on PAN in the CLIM_2000 simulation, where large reductions are simulated at the surface over the continents and throughout
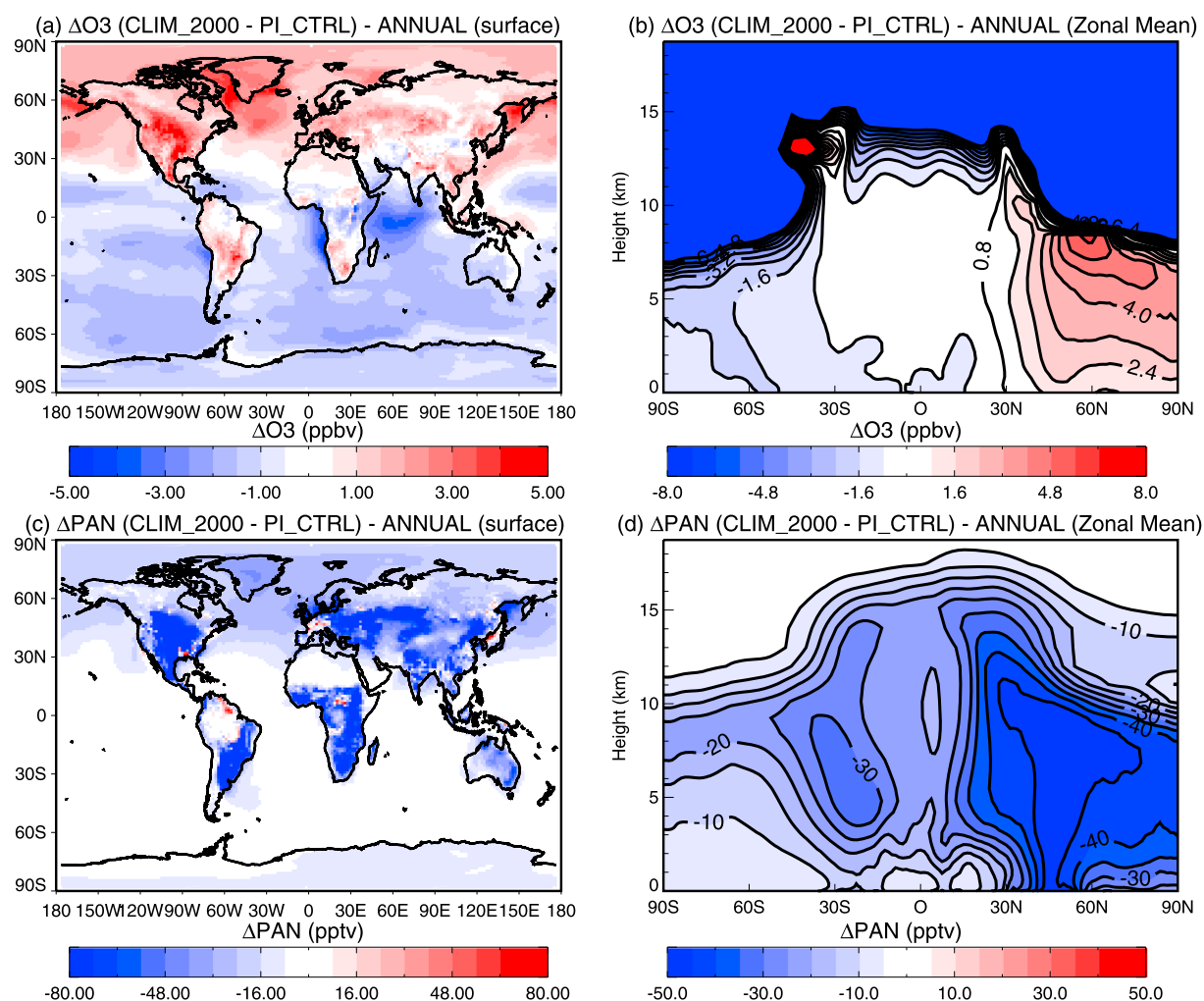
Figure 9. As in Figure 5 except for the CLIM_2000 versus PI_CTRL scenarios. Note the different scale on ozone changes.

the troposphere. The strong temperature dependence of the PAN lifetime [*Singh*, 1987] means that under warmer present-day climate conditions, its tropospheric loss rate is enhanced. This effect acts to enhance the effects of reductions in isoprene emissions under enhanced CO_2 and vegetation change to produce larger PAN decreases throughout the troposphere. Figure 6 shows that the influence of the PAN reductions on surface NO_x concentrations follows a similar pattern to that seen under the VEG_2000 scenario, due to the effects of reduced isoprene emissions and PAN formation as discussed in section 3.2.1. This results in two different effects dependent on location. Under the 1865 emissions scenario, areas over land are typically in a low NO_x environment, and therefore, the enhancement of surface NO_x concentrations (Figure 6) combine with the effects of reduced dry deposition and reduced isoprene emissions to lead to enhancements of surface ozone concentrations. This likely contributes to the rise in modeled surface ozone due to the change in model climate between the CLIM_2000 and PI_CTRL scenarios, an effect shown in previous studies [*Jacob and Winner*, 2009; *Fiore et al.*, 2012]. In contrast, the effects of reduced PAN concentrations result in large reductions in ozone in the remote SH and tropics of up to 4 ppbv. Ozone reductions in regions remote from NO_x sources are also enhanced by larger water vapor abundances in the present-day climate of the CLIM_2000 simulation.

The effect of CO_2 fertilization on vegetation likely also contributes to the larger tropospheric ozone concentrations under the CLIM_2000 scenario. As recently suggested by *Wu et al.* [2012] and *Tai et al.* [2014], higher CO_2 can enhance plant productivity increasing LAI and thus change dry deposition and bVOC emissions, which in the future may have comparable impacts on ozone concentrations as the changing climate itself. As leaf phenology is determined online in our simulations, and the CLIM_2000 scenario is driven using a higher CO_2 concentration representative of the near present day, the changes in LAI will include the impacts of

Table 3. Simulated Changes in Tropospheric Ozone Burden Between Each Model Scenario and the PI_CTRL Scenario[a]

Model Scenario[b]	Ozone Burden (Tg O_3)	ΔBurden (Tg O_3)	ΔTotal Column Ozone (DU)
PI_CTRL	203.7 ± 9.4	–	–
VEG_2000	200.4 ± 8.8	−3.3	−0.2
CLIM_2000	205.0 ± 9.3	1.3	0.2
CO2_DD	204.5 ± 10.6	0.8	0.1
CO2_DDBVOC	204.1 ± 10.9	0.4	0.0
PD_2000	292.9 ± 18.4	89.2	8.1

[a]All values are global annual averages. For reference the total column ozone for the PI_CTRL and PD_2000 simulations are 26.9 DU and 35.0 DU, respectively.
[b]For reference the values from ACCMIP are 337 ± 23 Tg O_3, 98 ± 17 Tg O_3, and 8.4 ± 1.3 DU for ozone burden, ΔBurden, and ΔTotal column ozone, respectively [*Young et al.*, 2013; *Stevenson et al.*, 2013]. The ±values for our results are ±standard deviation on the annual burden value.

CO_2 fertilization. Therefore, the response of ozone concentrations to CO_2-driven LAI increase will be included in this scenario; however, we have not isolated it explicitly in this study.

4. Impacts of Changing Atmospheric Chemistry-Vegetation Interactions on Free Tropospheric Ozone Distributions and Implications for Radiative Effect

Our simulations show that the sensitivities of midnineteenth century ozone to changes in the vegetation cover only and to changes in CO_{2Veg} are of similar magnitude but of opposite sign in terms of their effects on high latitude and tropical midtropospheric ozone. The effects of increasing CO_2 on stomatal conductance and on isoprene emissions both produce increases in continental surface ozone concentrations, due to a reduction in the deposition sink and isoprene ozonolysis sink of ozone. The effects of the reduced isoprene on PAN concentrations are larger and opposite in sign to the impacts of the CO_2 reduction in dry deposition, resulting in reduced PAN transport to remote regions and less ozone production. This effect also produces a large reduction in tropical UT ozone in response to both the land cover and CO_2 changes. Combining these changes in land cover and CO_2 with changes in climate between midnineteenth century and present day produces increases in tropospheric ozone and the largest increases in surface ozone throughout the Northern Hemisphere. This is a combined response to CO_2-induced and land cover-induced changes in isoprene emissions, reducing the isoprene ozonolysis ozone sink over the continents, and climate-driven reductions in stomatal conductance compounding reductions due to CO_2 increases. This results in further reduction in the dry deposition sink.

The changes in the tropospheric ozone burden between each of our scenarios and the PI_CTRL simulation are shown in Table 3. The simulations indicate a change in the modeled ozone burden of between −3.3 Tg (1.6%) under the VEG_2000 scenario to 1.3 Tg (0.6%) under the CLIM_2000 scenario. Using interannual standard deviation from our model runs, we estimate a range in variability on our estimates of the tropospheric ozone burden of between 8.7 Tg (4.4%) for the VEG_2000 scenario and 10.9 Tg (5.3%) for the CO2_DDBVOC scenario. Overall, this shows that the sensitivities of tropospheric ozone (in the midnineteenth century) to different treatments of atmospheric chemistry-vegetation interactions are smaller than the interannual variability. In this study we have shown that uncertainties arising from assumptions regarding the representations of atmospheric chemistry-vegetation can add to this variability in our best estimate of atmospheric conditions in the midnineteenth century which further stresses the case for better representation of these processes in Earth System models.

To put our work into context of previous studies, we also calculated our best estimate of the change in tropospheric ozone burden between the midnineteenth century and the present day (PI_CTRL versus PD_2000 scenarios), which is 89.2 Tg (43.7%). This is consistent with previous work which estimated a pre-industrial to present day change in ozone burden at 71.0–130.0 Tg [*Lamarque et al.*, 2005] and slightly higher than the ACCMIP study which estimated a modeled change in ozone burden of approximately 30% since 1850 [*Young et al.*, 2013]. Figure 10 shows the annually and zonally averaged changes in ozone between the PI_CTRL scenario and the present-day atmosphere (PD_2000). Our simulations show that ozone increases by at least 50% (around 12 ppbv) throughout the Northern Hemisphere between the midnineteenth century and the
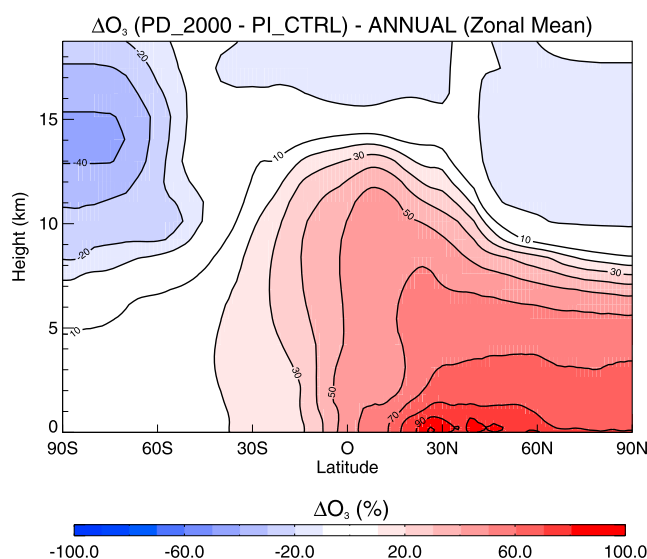
Figure 10. Percentage change of zonally averaged annual mean ozone between the PD_2000 and PI_CTRL scenarios.

present day. These increases approach 80–90% (around 18–20 ppbv) in the lower to mid-Northern Hemisphere troposphere with an approximate doubling of ozone seen at the surface between 30N and 60N. In the Southern Hemisphere ozone concentrations are shown to increase by 10–40% (2–5 ppbv) under all scenarios with the greatest changes seen around the tropics. In the upper troposphere, ozone increases are at least 10% (2 ppbv), with the greatest changes seen around the tropopause between 20N and 30N. The changes in this region are around 50% (16 ppbv). This is in agreement with recent results from ACCMIP [*Young et al.*, 2013] which showed midnineteenth century to present-day increases in tropospheric ozone of 5–20 ppbv in the lower troposphere in the Northern Hemisphere, 10-20 ppbv in the upper tropical troposphere, and 2–10 ppbv throughout the Southern Hemisphere troposphere.

Our best estimate for the tropospheric ozone radiative forcing (PD_2000 - PI_CTRL) is 0.264 W m^{-2}. This falls toward the lower end of previous estimates: 0.25–0.45 W m^{-2} by *Gauss et al.* [2006], 0.44 ± 0.13 W m^{-2} by *Skeie et al.* [2011], 0.29–0.53 W m^{-2} by the ACCMIP model intercomparison project [*Stevenson et al.*, 2013], 0.2–0.6 W m^{-2} by *Myhre et al.* [2013], and 0.32 W m^{-2} by *Rap et al.* [2015]. Our lower estimate could be due to the assumptions made regarding the prescribed anthropogenic emissions, as discussed further below. We also find some sensitivity of our forcing to the tropopause definition. Our choice of the 150 ppbv ozone contour to define the chemical tropopause means that some negative changes in lower stratospheric ozone between midnineteenth century and present day are included contributing to a damping of our tropospheric forcing estimate. However, this damping effect has been shown to be relatively small (approximately 5%) [*Stevenson et al.*, 2013].

To isolate the effect of midnineteenth century to present day change in vegetation on the tropospheric ozone radiative effect, we calculate the difference between the ozone radiative effects in the PI_CTRL and the VEG_2000 simulations. We find a −0.012 W m^{-2} trospospheric ozone radiative effect from using present-day land cover in the VEG_2000 scenario compared to the PI_CTRL scenario (Table 4). Thus, our results imply a negative impact on the tropospheric ozone radiative effect of −0.012 W m^{-2} (Table 4) due to this change. This sensitivity is an order-of-magnitude smaller than the negative tropospheric ozone effect of −0.13 W m^{-2} attributed to reductions in vegetation cover since the midnineteenth century by *Unger* [2014]. While the definition of the quantity calculated here is different from that of *Unger* [2014], the difference demonstrates the importance of experimental design in derivation of this sensitivity. The key difference between the definitions is the assumption regarding precursor emissions (particularly NO$_x$) from anthropogenic sources. Our radiative effect is calculated based on a change in vegetation from pre-industrial to year 2000, with emissions fixed at pre-industrial values. The previous estimate from *Unger* [2014] calculated the ozone forcing due to changes in land cover between pre-industrial and present day, using present-day emissions. The response of ozone and the associated radiative sensitivity is smaller in our simulations due to the land cover-induced changes in isoprene emissions occurring in lower NO$_x$ conditions (see schematic Figure 2).

Table 4. Simulated Changes in Tropospheric Ozone Radiative Effect (RE) Between Each Midnineteenth Century Scenario and the PI_CTRL Scenario

Model Scenario	$\Delta RE^a (W\ m^{-2})$
VEG_2000	−0.012
CLIM_2000	0.001
CO2_DD	0.001
CO2_DDBVOC	0.001

[a]For reference the midnineteenth century to present-day radiative forcing (PI_CTRL to PD_2000) is 0.264 W m^{-2}.

Our results highlight that the ozone radiative effect response to land cover change is dominated by the impacts of isoprene emission change on ozone in the upper troposphere, consistent with other studies which showed the importance of the tropical tropopause region [*Worden et al.*, 2011; *Riese et al.*, 2012; *Rap et al.*, 2015]. This response is largely controlled by the availability of NO$_x$ and processes that transport ozone and precursors to the upper troposphere. A key factor is the formation of PAN from isoprene oxidation and its transport to the tropical UT. The radiative impacts of ozone changes produced by the effects of changing CO$_2$ on isoprene emissions and dry deposition (CO$_{2Veg}$) between *PI* and present day (CO2_DDBVOC - PI_CTRL and CO2_DD - PI_CTRL) are very small (both 0.001 W m^{-2}). This is due to their much smaller impacts on ozone in the upper troposphere (Figures 7 and 8). It is, however, noted here that the relative sensitivity of the overall radiative forcing to changes in atmospheric chemistry-vegetation interactions is much smaller than the value of the forcing itself (0.264 W m^{-2}) with the largest contribution to this forcing coming from changes in anthropogenic emissions since 1865 [*Stevenson et al.*, 2013].

Previous studies have also noted the sensitivity of tropospheric ozone forcing to changes in natural emissions. *Mickley et al.* [2001] found that by increasing emissions of BVOCs from vegetation by 50% and increasing NO$_x$ emissions from soil and lightning, an instantaneous forcing of 0.72–0.80 W m^{-2} was calculated. This was approximately double the value of their standard pre-industrial simulation (0.44 W m^{-2}). Finally, uncertainties in biomass burning emissions of NO$_x$ in the pre-industrial along with potential uncertainties in soil emissions also lead to uncertainty in the pre-industrial tropospheric ozone burden. This may be particularly important, given the role of PAN in determining the response of remote surface and free tropospheric ozone to changes in isoprene emissions that we have highlighted. As the focus of this work is to isolate the effects of changing vegetation on isoprene emissions and dry deposition processes, we did not explicitly test the response to changing biomass burning and soil NO$_x$ emissions. However, we expect our results to also be sensitive to our assumption of midnineteenth century biomass burning emissions [*Pacifico et al.*, 2015; *Rap et al.*, 2015] and soil emissions of NO$_x$. This should be the subject of further investigation in future studies.

5. Conclusions

In this study, simulations using an Earth System Model showed that changes in dry deposition and isoprene emissions due to vegetation change (1865 to 2000) are shown to have a larger effect on surface ozone and the ozone burden (a 1.6% burden reduction from a control simulation) than those associated with the effects of the midnineteenth century to present-day change in atmospheric CO$_2$ concentration on isoprene emissions and dry deposition (a 0.4% burden increase from the control simulation). Our results also show that the response of ozone concentrations to vegetation and CO$_2$ changes is dominated by the impacts of changing isoprene emissions rather than changing dry deposition, agreeing with previous work [*Lamarque et al.*, 2005], in the low NO$_x$ regime of the midnineteenth century period.

Changes in surface vegetation cover since the midnineteenth century, and CO$_2$ suppression of isoprene emissions under present-day compared with midnineteenth century lead to decreases in global isoprene emissions of 19% and 21% respectively. The effect of land-cover driven decreases in isoprene since midnineteenth century is to increase surface ozone concentrations over the vegetated continents by up to 2 ppbv. The same decreases in isoprene result in lower surface ozone concentrations over non-vegetated and marine regions, due to decreased PAN formation and the subsequent decrease in transport of NO$_x$ to these regions, reducing ozone formation. When the land cover and CO$_2$ changes are combined with a change in

model climate, the ozone burden increases by 0.6% and surface ozone concentrations increase by up to 5 ppbv compared to the control simulation, with increases of 6–8 ppbv in the mid latitude upper troposphere.

Our simulations show that our best estimate of the midnineteenth century tropospheric ozone burden is 203.7 ± 9.4 Tg. We show that depending on assumptions regarding the model land PFT distribution, the atmospheric CO_2 mixing ratio controlling vegetation stomatal conductance and isoprene emission, and the model climate, this value can increase to 205.0 ± 9.2 Tg or be as low as 200.4 ± 8.8 Tg. The associated midnineteenth century to present-day change in ozone burden (present-day burden of 292.9 ± 18.4 Tg) is 89.2 Tg which leads to an associated radiative forcing of 0.264 W m^{-2}. Overall, the change in vegetation only (VEG_2000 – PI_CTRL) produces the largest differences (with reference to the control simulation) at the tropopause level resulting in a negative radiative forcing of -0.012 W m^{-2}. Changes in vegetation CO_2 exposure produce a much smaller impact at tropopause level, leading to a small radiative effect of $+0.001$ W m^{-2}.

As NO$_x$ emissions have varied dynamically between 1865 and 2000, our results coupled with those of *Unger* [2014] suggest that a shift to a higher NO$_x$ regime over this period means that sensitivities of the tropospheric ozone radiative effect to vegetation cover have likely increased by an order of magnitude. Overall, our simulations show that it is important to use the correct baseline land cover and that ideally simulated vegetation processes must also change interactively with dynamically changing NO$_x$ emissions.

Our results highlight the sensitivity of both the midnineteenth century surface ozone distribution and tropospheric ozone burden to assumptions regarding atmospheric chemistry-vegetation interactions, in particular isoprene emissions and their interaction with emissions of NO$_x$. Further work is required to understand how uncertainties in our knowledge of midnineteenth century NO$_x$ emissions interact with the sensitivities to vegetation cover presented here and the subsequent impacts on simulating pre-industrial ozone and ozone radiative forcing.

References

Anenberg, S. C., L. W. Horowitz, D. Q. Tong, and J. J. West (2010), An estimate of the global burden of anthropogenic ozone and fine particulate matter on premature human mortality using atmospheric modeling, *Environ. Health Perpectives*, *118*(9), 1189–1195, doi:10.1289/ehp.0901220.

Arneth, A., et al. (2007), Process-based estimates of terrestrial ecosystem isoprene emissions: Incorporating the effects of a direct co 2-isoprene interaction, *Atmos. Chem. Phys.*, *7*(1), 31–53, doi:10.5194/acp-7-31-2007.

Avnery, S., D. L. Mauzerall, and A. M. Fiore (2013), Increasing global agricultural production by reducing ozone damages via methane emission controls and ozone-resistant cultivar selection, *Global Change Biol.*, *19*(4), 1285–1299, doi:10.1111/gcb.12118.

Barket, D., et al. (2004), A study of the NO$_x$ dependence of isoprene oxidation, *J. Geophys. Res.*, *109*, D11310, doi:10.1029/2003JD003965.

Collins, W. J., S. Sitch, and O. Boucher (2010), How vegetation impacts affect climate metrics for ozone precursors, *J. Geophys. Res.*, *115*, D23308, doi:10.1029/2010JD014187.

Collins, W. J., et al. (2011), Development and evaluation of an Earth-System model—HadGEM2, *Geosci. Model Dev.*, *4*(4), 1051–1075, doi:10.5194/gmd-4-1051-2011.

Edwards, J. M., and A. Slingo (1996), Studies with a flexible new radiation code.1. Choosing a configuration for a large-scale model, *Q. J. R. Meteorol. Soc.*, *122*(531), 689–719, doi:10.1002/qj.49712253107.

Essery, R. L. H., M. J. Best, R. A. Betts, P. M. Cox, and C. M. Taylor (2003), Explicit representation of subgrid heterogeneity in a GCM land surface scheme, *J. Hydrometeorol.*, *4*(3), 530–543, doi:10.1175/1525-7541(2003)004<0530:EROSHI>2.0.CO;2.

Fiore, A. M., et al. (2012), Global air quality and climate, *Chem. Soc. Rev.*, *41*(19), 6663–6683, doi:10.1039/c2cs35095e.

Folberth, G., D. Hauglustaine, J. Lathiere, and F. Brocheton (2006), Interactive chemistry in the Laboratoire de Meteorologie Dynamique general circulation model: Model description and impact analysis of biogenic hydrocarbons on tropospheric chemistry, *Atmos. Chem. Phys.*, *6*, 2273–2319, doi:10.5194/acp-6-2273-2006.

Fu, Y., and A. P. K. Tai (2015), Impact of climate and land cover changes on tropospheric ozone air quality and public health in East Asia between 1980 and 2010, *Atmos. Chem. Phys.*, *15*(17), 10,093–10,106, doi:10.5194/acp-15-10093-2015.

Ganzeveld, L., and J. Lelieveld (1995), Dry deposition parameterization in a chemistry general circulation model and its influence on the distribution of reactive trace gases, *J. Geophys. Res.*, *100*, 20,999–21,012.

Gauss, M., et al. (2006), Radiative forcing since preindustrial times due to ozone change in the troposphere and the lower stratosphere, *Atmos. Chem. Phys.*, *6*, 575–599, doi:10.5194/acp-6-575-2006.

Gedney, N., P. Cox, R. Betts, O. Boucher, C. Huntingford, and P. Stott (2006), Detection of a direct carbon dioxide effect in continental river runoff records, *Nature*, *439*, 835–838, doi:10.1038/nature04504.

Giannakopoulos, C., T. P. Chipperfield, K. S. Law, and J. A. Pyle (1999), Validation and intercomparison of wet and dry deposition schemes using Pb-210 in a global three-dimensional off-line chemical transport model, *J. Geophys. Res.*, *104*(D19), 23,761–23,784, doi:10.1029/1999JD900392.

Guenther, A., P. Zimmerman, P. Harley, R. Monson, and R. Fall (1993), Isoprene and monoterpene emission rate variability—Model evaluations and sensitivity analyses, *J. Geophys. Res.*, *98*(D7), 12,609–12,617, doi:10.1029/93JD00527.

Guenther, A., T. Karl, P. Harley, C. Wiedinmyer, P. Palmer, and C. Geron (2006), Estimates of global terrestrial isoprene emissions using MEGAN (Model of Emissions of Gases and Aerosols from Nature), *Atmos. Chem. Phys.*, *6*, 3181–3210, doi:10.5194/acp-6-3181-2006.

Hauglustaine, D. A., and G. P. Brasseur (2001), Evolution of tropospheric ozone under anthropogenic activities and associated radiative forcing of climate, *J. Geophys. Res.*, *106*(D23), 32,337–32,360, doi:10.1029/2001JD900175.

Heald, C. L., M. J. Wilkinson, R. K. Monson, C. A. Alo, G. Wang, and A. Guenther (2009), Response of isoprene emission to ambient co 2 changes and implications for global budgets, *Global Change Biol.*, *15*(5), 1127–1140, doi:10.1111/j.1365-2486.2008.01802.x.

Hollaway, M. J., S. R. Arnold, A. J. Challinor, and L. D. Emberson (2012), Intercontinental trans-boundary contributions to ozone-induced crop yield losses in the Northern Hemisphere, *Biogeosciences*, *9*(1), 271–292, doi:10.5194/bg-9-271-2012.

Hurtt, G. C., et al. (2011), Harmonization of land-use scenarios for the period 1500–2100: 600 years of global gridded annual land-use transitions, wood harvest, and resulting secondary lands, *Clim. Change*, *109*(1–2), 117–161, doi:10.1007/s10584-011-0153-2.

Jacob, D. J., and D. A. Winner (2009), Effect of climate change on air quality, *Atmos. Environ.*, *43*(1), 51–63, doi:10.1016/j.atmosenv.2008.09.051.

Jones, C. D., et al. (2011), The HadGEM2-ES implementation of CMIP5 centennial simulations, *Geosci. Model Dev.*, *4*(3), 543–570, doi:10.5194/gmd-4-543-2011.

Klein Goldewijk, K., A. Beusen, and P. Janssen (2010), Long term dynamic modelling of global population and built-up area in a spatially explicit way: HYDE 3.1, *Holocene*, *20*, 565–573, doi:10.1177/0959683609356587.

Lamarque, J. F., P. Hess, L. Emmons, L. Buja, W. Washington, and C. Granier (2005), Tropospheric ozone evolution between 1890 and 1990, *J. Geophys. Res.*, *110*, D08304, doi:10.1029/2004JD005537.

Lamarque, J. F., et al. (2010), Historical (1850–2000) gridded anthropogenic and biomass burning emissions of reactive gases and aerosols: Methodology and application, *Atmos. Chem. Phys.*, *10*(15), 7017–7039, doi:10.5194/acp-10-7017-2010.

Lelieveld, J., et al. (2008), Atmospheric oxidation capacity sustained by a tropical forest, *Nature*, *452*, 737–740, doi:10.1038/nature06870.

Lombardozzi, D., J. P. Sparks, and G. Bonan (2013), Integrating o_3 influences on terrestrial processes: Photosynthetic and stomatal response data available for regional and global modeling, *Biogeosciences*, *10*(11), 6815–6831, doi:10.5194/bg-10-6815-2013.

Lombardozzi, D., S. Levis, G. Bonan, P. G. Hess, and J. P. Sparks (2015), The influence of chronic ozone exposure on global carbon and water cycles, *J. Clim.*, *28*(1), 292–305, doi:10.1175/JCLI-D-14-00223.1.

Loveland, T., B. Reed, J. Brown, D. Ohlen, Z. Zhu, L. Yang, and J. Merchant (2000), Development of a global land cover characteristics database and IGBP DISCover from 1 km AVHRR data, *Int. J. Remote Sens.*, *21*, 1303–1330, doi:10.1080/014311600210191.

Mickley, L. J., D. J. Jacob, and D. Rind (2001), Uncertainty in preindustrial abundance of tropospheric ozone: Implications for radiative forcing calculations, *J. Geophys. Res.*, *106*, 3389–3399, doi:10.1029/2000JD900594.

Monson, R., and R. Fall (1989), Isoprene emission from Aspen leaves—Influence of environment and relation to photosynthesis and photorespiration, *Plant Physiol.*, *90*(1), 267–274, doi:10.1104/pp.90.1.267.

Monson, R. K., et al. (2007), Isoprene emission from terrestrial ecosystems in response to global change: Minding the gap between models and observations, *Philos. Trans. R. Soc. London, Ser. A*, *365*(1856), 1677–1695, doi:10.1098/rsta.2007.2038.

Moxim, W. J., H. Levy, and P. S. Kasibhatla (1996), Simulated global tropospheric PAN: Its transport and impact on No_x, *J. Geophys. Res.*, *101*(D7), 12,621–12,638, doi:10.1029/96JD00338.

Myhre, G., et al. (2013), Anthropogenic and Natural Radiative Forcing, in *Climate Change 2013: The Physical Science Basis. Contribution of Working Group I to the Fifth Assessment Report of the Intergovernmental Panel on Climate Change*, edited by T. Stocker et al., Cambridge Univ. Press, Cambridge, U. K., and New York.

Niinemets, U., and Z. Sun (2015), How light, temperature, and measurement and growth [CO2] interactively control isoprene emission in hybrid aspen, *J. Exp. Bot.*, *66*(3), 841–851, doi:10.1093/jxb/eru443.

Niinemets, U., J. Tenhunen, P. Harley, and R. Steinbrecher (1999), A model of isoprene emission based on energetic requirements for isoprene synthesis and leaf photosynthetic properties for Liquidambar and Quercus, *Plant, Cell and Environment*, *22*, 1319–1335, doi:10.1046/j.1365-3040.1999.00505.x.

Niinemets, U., A. Arneth, U. Kuhn, R. K. Monson, J. Penuelas, and M. Staudt (2010a), The emission factor of volatile isoprenoids: Stress, acclimation, and developmental responses, *Biogeosciences*, *7*(7), 2203–2223, doi:10.5194/bg-7-2203-2010.

Niinemets, U., R. K. Monson, A. Arneth, P. Ciccioli, J. Kesselmeier, U. Kuhn, S. M. Noe, J. Penuelas, and M. Staudt (2010b), The leaf-level emission factor of volatile isoprenoids: Caveats, model algorithms, response shapes and scaling, *Biogeosciences*, *7*(6), 1809–1832, doi:10.5194/bg-7-1809-2010.

O'Connor, F. M., et al. (2014), Evaluation of the new UKCA climate-composition model—Part 2: The troposphere, *Geosci. Model Dev.*, *7*(1), 41–91, doi:10.5194/gmd-7-41-2014.

Pacifico, F., S. Harrison, C. Jones, and S. Sitch (2009), Isoprene emissions and climate, *Atmos. Environ.*, *43*(39), 6121–6135, doi:10.1016/j.atmosenv.2009.09.002.

Pacifico, F., et al. (2011), Evaluation of a photosynthesis-based biogenic isoprene emission scheme in JULES and simulation of isoprene emissions under present-day climate conditions, *Atmos. Chem. Phys.*, *11*(9), 4371–4389, doi:10.5194/acp-11-4371-2011.

Pacifico, F., G. A. Folberth, S. Sitch, J. M. Haywood, L. V. Rizzo, F. F. Malavelle, and P. Artaxo (2015), Biomass burning related ozone damage on vegetation over the amazon forest: A model sensitivity study, *Atmos. Chem. Phys.*, *15*(5), 2791–2804, doi:10.5194/acp-15-2791-2015.

Pacifico, F., G. A. Folberth, C. D. Jones, S. P. Harrison, and W. J. Collins (2012), Sensitivity of biogenic isoprene emissions to past, present, and future environmental conditions and implications for atmospheric chemistry, *J. Geophys. Res.*, *117*, D22302, doi:10.1029/2012JD018276.

Parrella, J. P., et al. (2012), Tropospheric bromine chemistry: Implications for present and pre-industrial ozone and mercury, *Atmos. Chem. Phys.*, *12*(15), 6723–6740, doi:10.5194/acp-12-6723-2012.

Pegoraro, E., A. Rey, E. G. Bobich, G. Barron-Gafford, K. A. Grieve, Y. Malhi, and R. Murthy (2004), Effect of elevated co_2 concentration and vapour pressure deficit on isoprene emission from leaves of Populus deltoides during drought, *Funct. Plant Biol.*, *31*(12), 1137–1147, doi:10.1071/FP04142.

Poschl, U., R. Von Kuhlmann, N. Poisson, and P. Crutzen (2000), Development and intercomparison of condensed isoprene oxidation mechanisms for global atmospheric modelling, *J. Atmos. Chem.*, *37*, 29–52, doi:10.1023/A:1006391009798.

Possell, M., C. N. Hewitt, and D. J. Beerling (2005), The effects of glacial atmospheric co_2 concentrations and climate on isoprene emissions by vascular plants, *Global Change Biol.*, *11*(1), 60–69.

Price, C., and D. Rind (1993), What determines the cloud-to-ground lightning fraction in thunderstorms?, *Geophys. Res. Lett.*, *20*(6), 463–466, doi:10.1029/93GL00226.

Ramankutty, N., and J. Foley (1999), Estimating historical changes in land cover: North American croplands from 1850 to 1992, *Global Ecol. Biogeogr.*, *8*, 381–396, doi:10.1046/j.1365-2699.1999.00141.x.

Rap, A., N. A. D. Richards, P. M. Forster, S. A. Monks, S. R. Arnold, and M. P. Chipperfield (2015), Satellite constraint on the tropospheric ozone radiative effect, *Geophys. Res. Lett.*, *42*(12), 5074–5081, doi:10.1002/2015GL064037.

Richards, J. (1990), Land transformation, in *The Earth as transformed by human action*, edited by B. Turner et al., pp. 163–178, Cambridge Univ. Press, Cambridge, U. K. and N. Y.

Riese, M., F. Ploeger, A. Rap, B. Vogel, P. Konopka, M. Dameris, and P. Forster (2012), Impact of uncertainties in atmospheric mixing on simulated UTLS composition and related radiative effects, *J. Geophys. Res.*, *117*, D16305, doi:10.1029/2012JD017751.

Rossow, W. B., and R. A. Schiffer (1999), Advances in understanding clouds from ISCCP, *Bull. Am. Meteorol. Soc.*, *80*(11), 2261–2287, doi:10.1175/1520-0477(1999)080<2261:AIUCFI>2.0.CO;2.

Ryerson, T., et al. (2001), Observations of ozone formation in power plant plumes and implications for ozone control strategies, *Science*, *292*(5517), 719–723, doi:10.1126/science.1058113.

Sanderson, M., W. Collins, C. Johnson, and R. Derwent (2006), Present and future acid deposition to ecosystems: The effect of climate change, *Atmos. Environ.*, *40*, 1275–1283, doi:10.1016/j.atmosenv.2005.10.031.

Shindell, D. T., G. Faluvegi, and N. Bell (2003), Preindustrial-to-present-day radiative forcing by tropospheric ozone from improved simulations with the GISS chemistry-climate GCM, *Atmos. Chem. Phys.*, *3*(5), 1675–1702, doi:10.5194/acp-3-1675-2003.

Sillman, S. (2000), Ozone production efficiency and loss of NO_x in power plant plumes: Photochemical model and interpretation of measurements in Tennessee, *J. Geophys. Res.*, *105*(D7), 9189–9202, doi:10.1029/1999JD901014.

Singh, H. B. (1987), Reactive nitrogen in the troposphere, *Environ. Sci. Technol.*, *21*(4), 320–327, doi:10.1021/es00158a001.

Sitch, S., P. M. Cox, W. J. Collins, and C. Huntingford (2007), Indirect radiative forcing of climate change through ozone effects on the land-carbon sink, *Nature*, *448*(7155), 791–U4, doi:10.1038/nature06059.

Skeie, R. B., T. K. Berntsen, G. Myhre, K. Tanaka, M. M. Kvalevåg, and C. R. Hoyle (2011), Anthropogenic radiative forcing time series from pre-industrial times until 2010, *Atmos. Chem. Phys.*, *11*(22), 11,827–11,857, doi:10.5194/acp-11-11827-2011.

Smith, R., D. Fowler, M. Sutton, C. Flechard, and F. Coyle (2000), Regional estimation of pollutant gas dry deposition in the UK: Model description, sensitivity analysis and outputs, *Atmos. Environ.*, *34*(22), 3757–3777, doi:10.1016/S1352-2310(99)00517-8.

Stevenson, D. S., et al. (2013), Tropospheric ozone changes, radiative forcing and attribution to emissions in the atmospheric chemistry and climate model intercomparison project (ACCMIP), *Atmos. Chem. Phys.*, *13*(6), 3063–3085, doi:10.5194/acp-13-3063-2013.

Strada, S., and N. Unger (2016), Potential sensitivity of photosynthesis and isoprene emission to direct radiative effects of atmospheric aerosol pollution, *Atmos. Chem. Phys.*, *16*(7), 4213–4234, doi:10.5194/acp-16-4213-2016.

Tai, A. P. K., M. V. Martin, and C. L. Heald (2014), Threat to future global food security from climate change and ozone air pollution, *Nat. Clim. Change*, *9*(4), 817–821, doi:10.1038/NCLIMATE2317.

Turner, I., R. Moss, and D. Skole (1993), Relating land use and global land cover change. A proposal for an IGBP-HDP Core Project, *IGBP Rep. no. 24, HDP Rep. No. 5*, The International Geosphere-Biosphere Programme. A study of global change and the Human Dimensions of Global Environmental Change Programme, Royal Swedish Academy of Sciences, Stockholm.

Unger, N. (2014), Human land-use-driven reduction of forest volatiles cools global climate, *Nat. Clim. Change*, *4*(10), 907–910, doi:10.1038/nclimate2347.

Val Martin, M., C. L. Heald, and S. R. Arnold (2014), Coupling dry deposition to vegetation phenology in the community Earth system model: Implications for the simulation of surface O_3, *Geophys. Res. Lett.*, *41*(8), 2988–2996, doi:10.1002/2014GL059651.

Van Dingenen, R., F. J. Dentener, F. Raes, M. C. Krol, L. Emberson, and J. Cofala (2009), The global impact of ozone on agricultural crop yields under current and future air quality legislation, *Atmos. Environ.*, *43*(3), 604–618, doi:10.1016/j.atmosenv.2008.10.033.

Wang, Y., J. A. Logan, and D. J. Jacob (1998), Global simulation of tropospheric O_3-NO_x-hydrocarbon chemistry: 2. Model evaluation and global ozone budget, *J. Geophys. Res.*, *103*(D9), 10,727–10,755, doi:10.1029/98JD00157.

Wang, Y. H., and D. J. Jacob (1998), Anthropogenic forcing on tropospheric ozone and OH since preindustrial times, *J. Geophys. Res.*, *103*(D23), 31,123–31,135, doi:10.1029/1998JD100004.

Wesely, M. (1989), Parameterization of surface resistances to gaseous dry deposition in regional scale numerical models, *Atmos. Environ.*, *23*(6), 1293–1304, doi:10.1016/0004-6981(89)90153-4.

Wilkinson, M. J., R. K. Monson, N. Trahan, S. Lee, E. Brown, R. B. Jackson, H. W. Polley, P. A. Fay, and R. Fall (2009), Leaf isoprene emission rate as a function of atmospheric CO_2 concentration, *Global Change Biol.*, *15*(5), 1189–1200, doi:10.1111/j.1365-2486.2008.01803.x.

Worden, H. M., K. W. Bowman, S. S. Kulawik, and A. M. Aghedo (2011), Sensitivity of outgoing longwave radiative flux to the global vertical distribution of ozone characterized by instantaneous radiative kernels from Aura-TES, *J. Geophys. Res.*, *116*, D14115, doi:10.1029/2010JD015101.

Wu, S., L. J. Mickley, J. O. Kaplan, and D. J. Jacob (2012), Impacts of changes in land use and land cover on atmospheric chemistry and air quality over the 21st century, *Atmos. Chem. Phys.*, *12*(3), 1597–1609, doi:10.5194/acp-12-1597-2012.

Young, P. J., A. Arneth, G. Schurgers, G. Zeng, and J. A. Pyle (2009), The CO_2 inhibition of terrestrial isoprene emission significantly affects future ozone projections, *Atmos. Chem. Phys.*, *9*(8), 2793–2803, doi:10.5194/acp-9-2793-2009.

Young, P. J., et al. (2013), Pre-industrial to end 21st century projections of tropospheric ozone from the atmospheric chemistry and climate model intercomparison project (ACCMIP), *Atmos. Chem. Phys.*, *13*(4), 2063–2090, doi:10.5194/acp-13-2063-2013.

Yue, X., and N. Unger (2014), Ozone vegetation damage effects on gross primary productivity in the United States, *Atmos. Chem. Phys.*, *14*(17), 9137–9153, doi:10.5194/acp-14-9137-2014.